Environmental Microbiology

ENVIRONMENTAL MICROBIOLOGY

BRIEF REPORT OPEN ACCESS

Shallow Hydrothermal Fluids Shape Microbial Dynamics at the Tagoro Submarine Volcano (Canary Islands, Spain)

Clàudia Pérez-Barrancos[1,2] | Eugenio Fraile-Nuez[1] | Juan Pablo Martín-Díaz[1,3] | Alba González-Vega[1] | José Escánez-Pérez[1] | María Isabel Díaz-Durán[1] | Carmen Presas-Navarro[1] | Mar Nieto-Cid[4] | Jesús María Arrieta[1]

[1]Centro Oceanográfico de Canarias, Instituto Español de Oceanografía, Consejo Superior de Investigaciones Científicas (IEO-CSIC), Santa Cruz de Tenerife, Spain | [2]Universidad de Las Palmas de Gran Canaria (ULPGC), Las Palmas de Gran Canaria, Spain | [3]Universidad de La Laguna (ULL), San Cristóbal de La Laguna, Spain | [4]Centro Oceanográfico de A Coruña, Instituto Español de Oceanografía, Consejo Superior de Investigaciones Científicas (IEO-CSIC), A Coruña, Spain

Correspondence: Jesús María Arrieta (jesus.arrieta@ieo.csic.es)

Received: 16 July 2024 | **Revised:** 18 January 2025 | **Accepted:** 23 January 2025

Funding: This work was supported by Ministerio de Ciencia, Innovación y Universidades (20223PAL005), Agencia Estatal de Investigación (CTM2017-84735-R, PID2021-125368NB-I00 and PRE2018-083800) and Instituto Español de Oceanografía (IEO-CSIC-2015-2026).

Keywords: fertilisation experiments | hydrothermal fluxes | microbial abundance | microbial composition | microbial structure | underwater volcano

ABSTRACT

Shallow underwater hydrothermal systems are often overlooked despite their potential contribution to marine diversity and biogeochemistry. Over a decade after its eruption, the Tagoro submarine volcano continues to emit heat, reduced compounds, and nutrients into shallow waters, serving as a model system for studying the effects of diffuse hydrothermal fluids on surface microbial communities. The impact on both phytoplankton and bacterial communities was examined through experimental manipulations mimicking dilution levels up to ~100 m from the primary crater of Tagoro. Chlorophyll *a* concentration doubled in the presence of hydrothermal products, with peak levels detected about a day earlier than in controls. Picoeukaryotes and *Synechococcus* cell abundances moderately increased, yet small eukaryotic phytoplankton ($\leq 5\,\mu m$) predominated in the hydrothermally enriched bottles. Dinoflagellates, diatoms, small green algae and radiolarians particularly benefited from the hydrothermal inputs, along with phototrophic and chemoautotrophic bacteria. Our results indicate that hydrothermal products in shallow waters enhance primary production driven by phototrophic microbes, potentially triggering a secondary response associated with increased organic matter availability. Additionally, protistan grazing and parasitism emerged as key factors modulating local planktonic communities. Our findings highlight the role of shallow submarine hydrothermal systems in enhancing local primary production and element cycling.

1 | Introduction

Shallow hydrothermal vents represent unique ecosystems where primary productivity is particularly supported by both chemosynthesis and photosynthesis. These vents are distributed worldwide, but have not received as much attention as their deep-sea counterparts (Price and Giovannelli 2017). The availability of light, together with the enrichment of nutrients and reduced chemical compounds through buoyant hydrothermal fluids, sustain intense microbial activity in surface seawaters capable of supporting higher trophic levels (Caramanna, Sievert, and Bühring 2021). However, the development of microbial communities is frequently subject to substantial variability due to tides, wind forcing and abrupt geodynamic events (Yücel et al. 2013). Previous studies have shown that shallow-water hydrothermal habitats often foster the growth of indigenous microorganisms, compared with deep-sea vents, which tend to host vent-specific taxa (Tarasov et al. 2005). Still, the activity

of seawater and vent-derived microbes and their influence on geochemical fluxes is not well understood, especially in low-temperature diffuse vents (Wankel et al. 2011; Olins et al. 2013). Recent studies highlight shallow diffuse vents as important contributors to the total thermal and chemical flux entering the ocean (Martín-Díaz et al. 2024). These lower-temperature vents (< 100°C) display a mixture of oxygen-rich seawater with reduced chemicals from hydrothermal inputs, resulting in a wide range of microbial habitats. This diversity likely supports higher rates of primary productivity and biological biomass compared to high-temperature vents (Tarasov et al. 2005; Olins et al. 2013). Nonetheless, the specific environmental factors that influence the abundance and activity of microbes in these habitats require further investigation.

The Tagoro submarine volcano, located only 1.8 km off the southern coast of El Hierro island (Canary Islands, Spain) and with a summit 89 m below the sea surface (Fraile-Nuez et al. 2012, 2018), represents a unique opportunity to expand our understanding of the impacts of shallow underwater eruptive and degassing processes on the marine environment. It has indeed been monitored by the Spanish Institute of Oceanography (IEO-CSIC) for over a decade, with more than 30 multidisciplinary oceanographic cruises conducted since the early eruptive phase in October 2011 to the current active venting phase. Fieldwork strategies for the detection and monitoring of active hydrothermal sources in the area have been most recently detailed in González (2023). Major efforts have been focused on the geomorphological characterisation of its volcanic structure (Álvarez-Valero et al. 2023; Vázquez et al. 2023), as well as on the physical–chemical perturbations near the bottom and throughout the adjacent water column (Fraile-Nuez et al. 2012, 2018, 2023; Santana-Casiano et al. 2013, 2016; González-Vega et al. 2020, 2022, 2023; Martín-Díaz et al. 2024). Currently, the hydrothermal field covers an area of 7600 m^2, extending from the main hydrothermal crater at 127 m depth to the summit (Martín-Díaz et al. 2024). Thousands of small and diverse hydrothermal vents, irregularly dispersed across the venting field, inject warm waters, reduced compounds, trace metals and inorganic nutrients (Santana-Casiano et al. 2013; Martín-Díaz et al. 2024). The waters surrounding Tagoro exhibit significant physical–chemical anomalies, with an increase in potential temperature of 2.55°C, a decrease in salinity of 1.02 units, a decrease in density of 1.43 kg m^{-3} and a decrease in pH of 1.25 units (Fraile-Nuez et al. 2018), yet anomalies in oxygen profiles are no longer found (González-Vega et al. 2022). Significant enrichments of dissolved inorganic nutrient concentrations persist in the vicinity of Tagoro (González-Vega et al. 2020, 2023; Martín-Díaz et al. 2024), with large amounts of hydrothermal iron ores depositing in the sediments (González et al. 2020), while large concentrations of reduced iron also remain dissolved and bioavailable (Santana-González et al. 2017).

The progressive recovery of the ecosystem after the devastating eruptive process of Tagoro (October 2011–March 2012) was particularly noticeable in benthic and pelagic communities (Ariza et al. 2014; Danovaro et al. 2017; González et al. 2020; Sotomayor-García et al. 2023). The post-eruptive phase offered more hospitable conditions for marine organisms to thrive, in which microorganisms involved in iron, sulfur and methane metabolism were able to grow (González et al. 2020; Sotomayor-García et al. 2020), including novel microbes such as *Candidatus* Thiolava veneris (Danovaro et al. 2017). The recuperation also involved early colonisers such as small hydrozoan colonies with a high diversity of annelids, arthropods, cnidarians and molluscs, together with some sponges and echinoderms (Sotomayor-García et al. 2023).

Few studies have yet investigated the ecological impact of Tagoro on surface planktonic communities, particularly during the current degassing stage (Ferrera et al. 2015; Gómez-Letona et al. 2018; Fernández de Puelles et al. 2021). Higher abundances of zooplankton in waters affected by the volcano have been described (Fernández de Puelles et al. 2021). Researchers especially observed a higher presence of non-calanoid copepods, along with a decline in the diversity of the copepod community. High concentrations of inorganic nutrients and iron injected from Tagoro into the water column are expected to favour the proliferation of photosynthetic communities in Tagoro (Santana-Casiano, González-Dávila, and Fraile-Nuez 2017; González-Vega et al. 2020), as it has been often observed in other shallow-water systems around the world (e.g., Tarasov 2006; Ardyna et al. 2019; Schine et al. 2021). However, so far no clear evidence of fertilisation (i.e., the enhancement of primary productivity due to nutrient enrichment) has been found around Tagoro (Gómez-Letona et al. 2018). This is possibly due to the difficulty in distinguishing hydrothermally enriched water masses from unaffected background seawater, which makes it challenging to detect a potential fertilisation signal.

In this study, an experimental approach was employed to assess the potential effects of diffuse hydrothermal emissions on surface marine microbial communities (phytoplankton and bacteria) at the Tagoro submarine volcano. Microbial responses to proportional increases of hydrothermally enriched seawater and vent fluids were assessed in terms of cell abundances, diversity and community structure. The experimental treatments were designed to replicate the natural dilution of vent fluids in the vicinity of Tagoro. Dilution levels simulated in situ observations obtained over 9 years using dissolved inorganic silicate as a proxy for hydrothermal emissions in the area. The potential dispersion of hydrothermal fluids to the illuminated surface waters was assessed by examining mixed layer depth (MLD) estimates derived from in situ hydrographic data collected over the past decade. Together, our research enhances our understanding of the dynamics of surface marine microbial communities, their potential interactions with higher trophic levels and their implications for local productivity, nutrient cycling and carbon sequestration around shallow hydrothermal venting areas.

2 | Materials and Methods

2.1 | Experimental Addition of Hydrothermal Fluids

This research was developed as part of the VULCANA monitoring program from the Spanish Institute of Oceanography (IEO-CSIC). Two hydrothermal fluid addition experiments were conducted in April (spring) and two more in October (autumn) 2021, each lasting 8–10 days, on board the R/V *Ángeles Alvariño* at the Tagoro submarine volcano (El Hierro, Spain).

Seawater samples were collected at two vertical hydrographic stations using a rosette frame equipped with 24 Niskin bottles, each with a 12-L capacity, a dissolved oxygen sensor, a pH/oxidation–reduction potential (ORP) sensor, a fluorometer and two turbidimeters, coupled to an SBE 911-plus (Sea-Bird Electronics) CTD sensor (conductivity, temperature and depth). Calibration of all sensors was conducted before and after each oceanographic cruise. An outline of the experiments is provided in Figure 1. Briefly, unaffected seawater was collected at a reference station located outside the area of influence of Tagoro (~127 m depth; 27°39.000′ N, 17°54.587′ W; Figure 2A) and was used to fill the 5-L polycarbonate bottles designated as experimental bottles. All plasticwares were acid-washed with 0.12 N HCl for 30 min, and rinsed three times with sample water. A few hours later, hydrothermally enriched seawater samples were collected from the primary

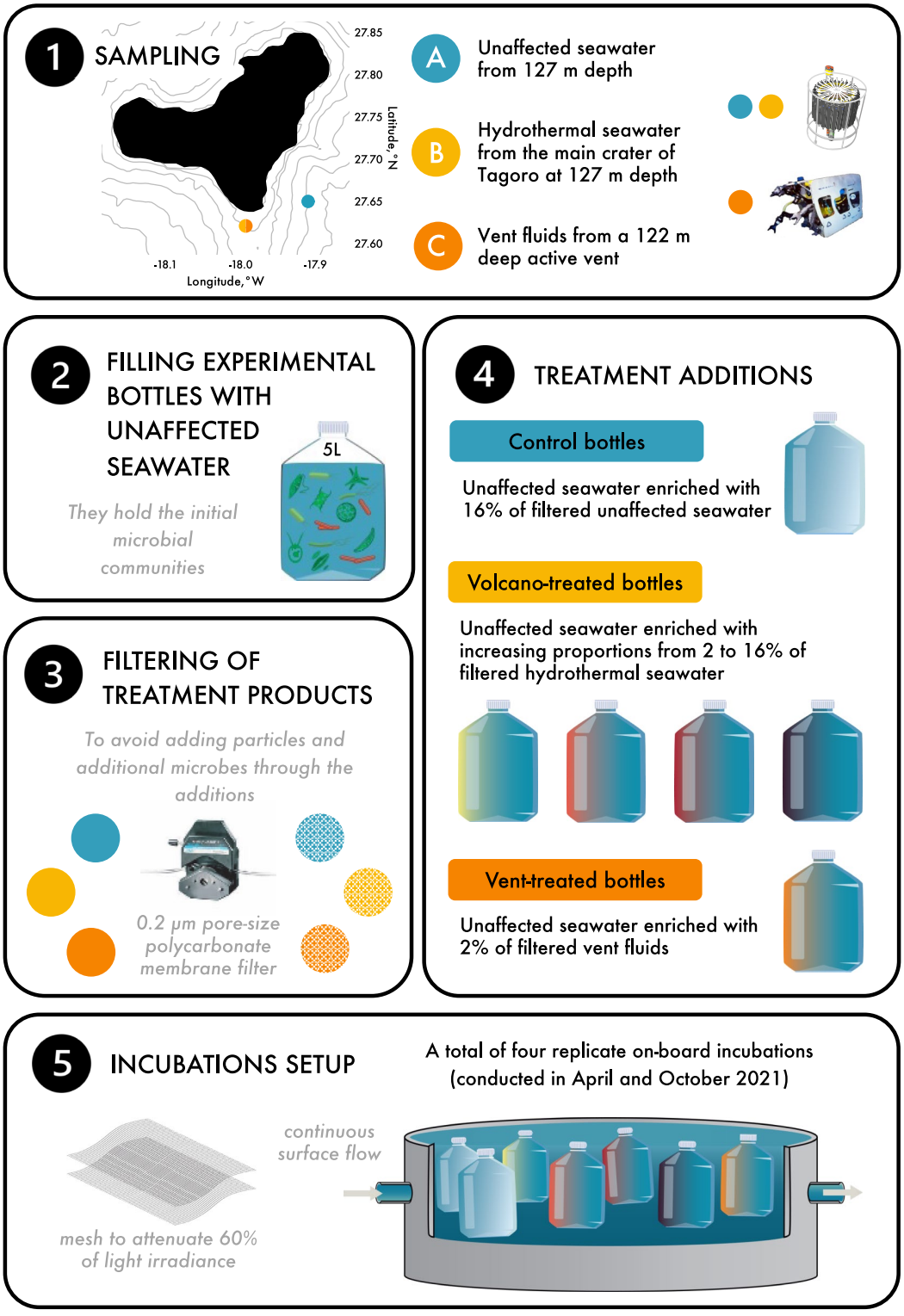

FIGURE 1 | Overview of the setup used to test the effect of hydrothermal fluid additions at Tagoro submarine volcano (El Hierro, Spain).

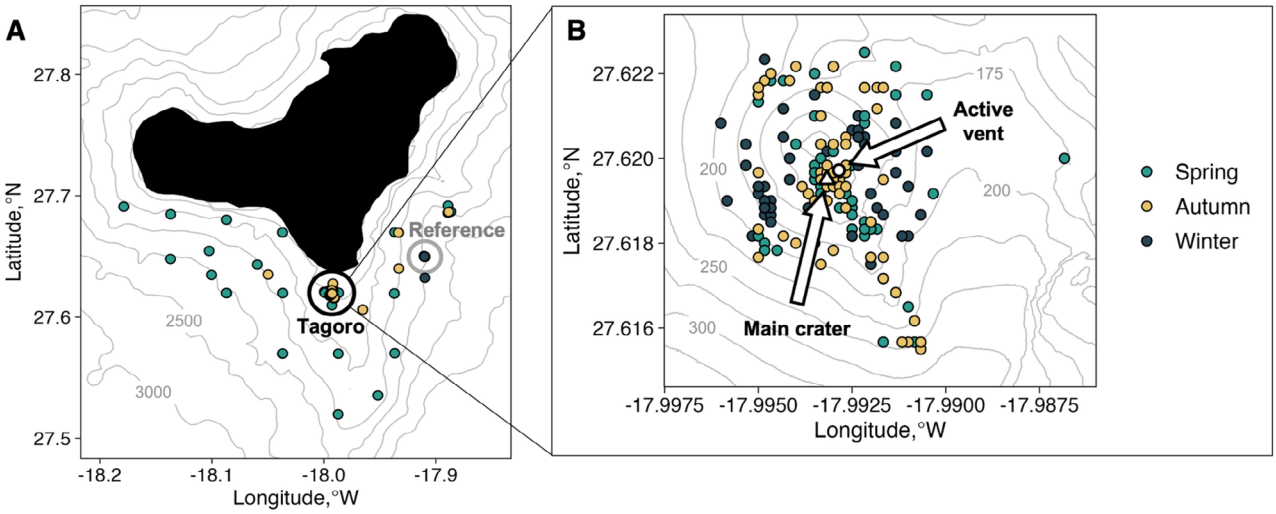

FIGURE 2 | (A) Hydrographic stations sampled south of El Hierro during VULCANA cruises from 2013 to 2023. Point colours indicate the season of sampling: Spring (green), autumn (yellow) and winter (blue). Circled areas highlight the reference station (grey) and the Tagoro hydrothermal field (black). Contours are displayed with an interval of 500 m. (B) Map of the hydrothermal field, with contour intervals of 25 m, showing the location of the main crater of Tagoro (white triangle), and the active vent sampled (white circle).

crater of Tagoro (~127 m depth; 27°37.184′ N, 17°59.184′ W; Figure 2B) at locations where simultaneous decreases in pH and increases in temperature were detected compared to the surrounding waters. Hydrothermal samples were then filtered through 47 mm diameter, 0.2 μm pore-size polycarbonate membrane filters using a peristaltic pump and homogenised in a 20-L polycarbonate bottle before being added to the experimental bottles. Each experiment consisted of two replicate control bottles filled with unaffected seawater and four bottles filled with unaffected seawater enriched with increasing volumes of filtered hydrothermal seawater (from 2% to 16% of the total volume), hereafter referred to as 'volcano-treated'. Controls were also subjected to an addition of 16% filtered unaffected seawater to account for any artefacts introduced by the handling of hydrothermal water samples.

An additional treatment, labelled as 'vent-treated', was introduced during the October 2021 cruise using vent fluids collected directly from an active hydrothermal vent near the primary crater (~122 m depth; 27°37.1832′ N, 17°59.5712′ W; Figure 2B). Sampling was performed using a remotely operated vehicle (ROV, *Liropus 2000*) equipped with a piston-driven suction system and with a HOBO TidbiT water temperature data logger (Onset Computer Corp.). Vent fluids were filtered (0.2 μm pore-size polycarbonate membrane filter) and homogenised in a 20-L polycarbonate bottle prior to the addition. In this instance, two replicate bottles filled with unaffected seawater were enriched with filtered vent fluids to 2% of the total volume. These vent-treated bottles were then incubated with the rest of experimental bottles for 9 days. Throughout the manuscript we will use the term 'treated' to refer to both volcano and vent-treated bottles.

The ratios of dilution were determined based on previous reports of dissolved silicate concentrations in the area of influence of Tagoro (González-Vega et al. 2020), where this nutrient was found to be a tracer of hydrothermal activity. These authors reported median and maximum enrichments of 4.6- and 16.3-fold, respectively, in the water column during the degassing stage compared to unaffected waters. We designed our experiments to cover a range from 2% to 16% of hydrothermal fluid addition, corresponding to the dissolved silicate concentrations in seawater previously observed adjacent to the main hydrothermal sources of Tagoro. In the case of vent fluids, previous studies observed a median 243.4-fold enrichment compared to unaffected waters (González-Vega et al. 2020). Thus, we simulated an addition of at least 2% of vent fluids, expected to result in the ~4-fold enrichment levels found in the water column.

The experimental bottles were incubated in 600 L high-density polyethylene tanks on-deck. Each tank was subjected to a continuous flow of surface seawater to provide sea surface temperature conditions and was covered with a double layer of optically neutral wire mesh reducing light intensity by 60%. Seawater temperature and light intensity were continuously monitored using a HOBO Pendant Temp/Light data logger (Onset Computer Corp.). Sampling was mostly performed at the beginning and end of experiments, although some parameters like chlorophyll *a* concentration and microbial abundances were sampled daily.

2.2 | Estimation of Dilution Levels

The dilution levels reproduced in our experiments were estimated from the exponential decay of dissolved silicate concentrations with increasing distance to the primary crater. This was determined using 145 water column samples collected at depths of approximately 120 and 130 m between March 2014 and February 2023 (Figure 4B and Table S1). A non-linear regression using the least-squares fitting method was applied, resulting in an exponential decay equation that best described the observed data at Tagoro (Figure 4B). This equation was then used to compute the corresponding distances (i.e., dilution levels) for each experimental treatment based on

their dissolved silicate concentrations. The uncertainty of the model was evaluated using the standard error and 95% confidence intervals. This data compilation represents the largest dataset published to date on the continuous silicate enrichment at the active Tagoro hydrothermal field throughout its degassing phase.

2.3 | Estimation of the Seasonal Mixed Layer Depth

The potential of hydrothermal fluids from Tagoro to reach shallower layers throughout the euphotic zone was assessed through seasonal MLD estimates. Hydrographic profiles of temperature, salinity and pressure collected between March 2013 and February 2023 as part of the VULCANA research project were used to derive the MLD south of El Hierro (latitudes between 27.46983° N and 27.69200° N). Most profiles were acquired using an SBE 911-plus CTD, with an average vertical resolution of 1 dbar, a temperature precision of 0.001°C and a conductivity precision of 0.0003 S m^{-1}.

Only profiles extending to depths below 100 m were used, resulting in a total of 1070 profiles in our study region. About 485 of the profiles were collected in spring (March–June), 154 in autumn (September–November) and 431 in winter. Moreover, about 75% of the profiles were acquired above the Tagoro hydrothermal field (Figure 2B) and another 12% were collected at the reference station southeast of El Hierro (Figure 2A). Examples of typical spring, autumn and winter profiles at both sites are shown in Figure S1, along with their seasonal median MLD estimates. Given the differences in sampling frequency across seasons and the large variability in MLD estimates, we chose to represent seasonal median values to provide a more accurate representation of the central tendency for each season (Figures 2A and 3).

The MLD was defined as the depth at which the maximum difference in the potential density profile was observed. Potential density is a valuable parameter for estimating the vertically homogeneous mixed layer, as it depends on both temperature and salinity and includes a correction for pressure effects (de Boyer Montégut et al. 2004). Based on the method of Lorbacher et al. (2006), we identified the maximum potential density gradient in each profile. This approach enabled the identification of the maximum depth reached by recent mixing events.

2.4 | Dissolved Inorganic Nutrient Concentrations

Seawater samples (12 mL per duplicate) were collected in polypropylene tubes and frozen at −20°C until analysis. Nutrient concentrations were analysed by colorimetric determination using a four-channel automatised air-segmented continuous flow system SEAL AA3 AutoAnalyzer. Nitrate plus nitrite ($NO_3^- + NO_2^-$) were determined by the copper–cadmium reduction method, whereas phosphate (PO_4^{3-}) and silicate ($Si(OH)_4$) were determined by the molybdate blue method (Aminot and Kérouel 2007). The instrumental limit of quantification was 0.02 μM for $NO_3^- + NO_2^+$, 0.01 μM for PO_4^{3-} and 0.04 μM for $Si(OH)_4$.

2.5 | Dissolved Organic Carbon and Nitrogen Concentrations

Seawater samples (30 mL per duplicate) were collected in combusted (450°C for 12 h) amber glass vials at the beginning and end of the October 2021 incubations and preserved at −20°C until analysis. After acidification with H_3PO_4 to pH <2, dissolved organic carbon (DOC) and total dissolved nitrogen (TDN) were measured using a Shimadzu TOC-V organic carbon analyser coupled to a TNM-1 total nitrogen unit. The system

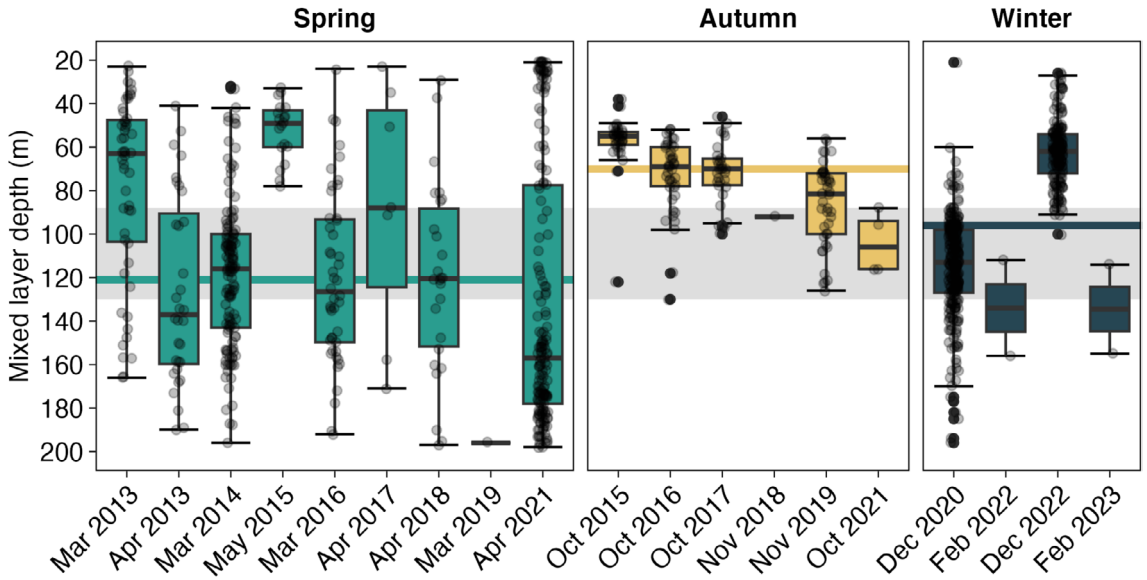

FIGURE 3 | Mixed layer depth (MLD, m) estimates per cruise conducted south of El Hierro. Grey dots show the actual observations and boxplots show the median, and first (upper) and third (lower) quartiles. Outliers are marked as black dots. Horizontal bold lines indicate the median MLD for spring ($n = 485$ profiles), autumn ($n = 154$) and winter ($n = 431$). Grey shaded areas indicate the depth of active hydrothermal venting at Tagoro following Martín-Díaz et al. (2024).

was standardised daily with a mixture of potassium hydrogen phthalate and glycine.

2.6 | Chlorophyll *a* Concentrations and Phytoplankton Growth Estimates

Seawater samples for chlorophyll *a* (250 mL) were filtered onboard through 25 mm diameter, 0.7 μm pore size Whatman GF/F glass fibre filters and stored at −20°C until analysis. Pigments were extracted overnight in 90% acetone at −20°C in the dark (Holm-Hansen et al. 1965). Chlorophyll *a* concentrations were determined fluorometrically on an Aquafluor (Turner Designs) handheld fluorometer.

The apparent phytoplankton growth rates (μ) were estimated from changes in chlorophyll *a* concentration, assuming an exponential growth model

$$N_t = N_0 e^{\mu t}$$

where N_0 is the population size at the beginning of a time interval, N_t is the population size at the end of the time interval and μ is the proportional rate of change expressed per unit time (t^{-1}). Note that losses incurred through viral lysis, grazing or other factors were not accounted for. Consequently, the actual growth rates of phytoplankton in our experiments are expected to be higher than the estimates provided in this study.

2.7 | Picophytoplankton and Heterotrophic Bacteria Abundances

Seawater samples for microbial abundance (1 mL per duplicate) were preserved with paraformaldehyde (1% final concentration), fixed for 30 min in the dark at 4°C, flash frozen in liquid nitrogen and stored at −80°C until processed. Once in the laboratory, samples were thawed, diluted in Tris-EDTA 1× buffer (pH 8) and 200 μL aliquots were stained in the dark for 10 min with SYBR Green I prior to analysis. Picophytoplankton and heterotrophic bacteria (≤2 μm) were counted using a CytoFLEX flow cytometer (Beckman Coulter) fitted with 405, 488 and 561 nm lasers. Autotrophic cells were readily detected in seawater samples by the fluorescence of their photosynthetic pigments. Specifically, *Synechococcus* were differentiated from *Prochlorococcus* by their emission of orange fluorescence and generally larger cell size, whereas picoeukaryotes were detected by their larger side scatter and red fluorescence and absence of orange fluorescence (Marie et al. 1997). Heterotrophic bacteria were detected in SYBR Green I–stained samples and characterised by the presence of green fluorescence and lack of red or orange fluorescence.

2.8 | Microbial Community Structure

Seawater samples for 16S and 18S rRNA gene sequencing (~1 L) were filtered through a 0.20-μm pore-size filter using a peristaltic pump and stored at −80°C.

The isolation of genomic DNA and the preparation of sequencing libraries were performed at the Canary Islands Oceanographic Center (IEO-CSIC) research facilities. DNA was extracted following the phenol–chloroform method (Sambrook and Russell 2001). Primers 515F (GTGYCAGCMG CCGCGGTAA) (Parada, Needham, and Fuhrman 2016) and 806R (GGACTACNVGGGTWTCTAAT) (Apprill et al. 2015) were used to target the V4 region of the prokaryotic 16S rRNA (~390 bp). Each PCR reaction (20 μL) contained 10 μL of AccuStart II PCR SuperMix (2×), 0.6 μL of each 20 μM primer stock, 3.8 μL of water and 5 μL of DNA template. The PCR program comprised an initial denaturation step at 94°C during 3 min, 35 amplification cycles, each consisting of 94°C for 45 s, 50°C for 60 s and 72°C for 90 s, a final elongation step at 72°C for 10 min and cooling to 4°C. On the other hand, the V4 region of the eukaryotic 18S rRNA (~260 ± 50 bp) was targeted using TAReuk454FWD1 (CCAGCASCY GCGGTAATTC) and TAReukREV3 (ACTTTCGTTCTTG ATYRA) primer set (Stoeck et al. 2010). PCR reactions were set up as previously described for the 16S rRNA gene. On this occasion, the PCR program consisted of an initial denaturation step at 94°C for 3 min, 15 amplification cycles of 94°C for 45 s, 53°C for 30 s and 72°C for 30 s, followed by 20 additional amplification cycles, each consisting of 94°C for 45 s, 48°C for 30 s and 72°C for 30 s, a final elongation step at 72°C for 10 min and cooling to 4°C. For each library, amplified PCR products were cleaned, indexed and quantified following the Illumina 16S metagenomic sequencing library preparation protocol. Equimolar amounts of cleaned-up indexed samples were pooled and paired-end sequenced (2 × 300) on an Illumina MiSeq platform (Macrogen, Korea). Sequence data (demultiplexed sequences with primers and adapters) is available at NCBI (https://www.ncbi.nlm.nih.gov/sra) under ID Number PRJNA1098582.

After primer removal with cutadapt v1.18, amplicon datasets were processed using the DADA2 v1.28 pipeline (Callahan et al. 2016) with trimming and filtering parameters estimated through FIGARO (Weinstein et al. 2019). The obtained combinations were *truncLen* 216,143 and *maxEE* 1 for the prokaryotic 16S rRNA dataset, and *truncLen* 230,200 and *maxEE* 2 for the eukaryotic 18S rRNA dataset. Sample inference was performed by pooling together sequences from all samples. An amplicon sequence variant (ASV) table was obtained for each dataset, with chimera removal using the consensus approach. Prokaryotic taxonomic assignment was performed according to Silva SSU Version 138.1, and sequences classified as eukaryote, mitochondria or chloroplast were discarded from the 16S rRNA dataset. Eukaryotic taxonomy was determined using the PR^2 database (Guillou et al. 2013), and any bacterial and archaeal sequences were excluded from the 18S rRNA dataset. Opisthokonta sequences, comprising 1.5% of the eukaryotic 18S rRNA dataset, were also removed from the analysis. They were predominantly classified within the Metazoa and Pseudofungi divisions, including a broad group of animals and heterokonts not relevant to the purpose of our study, with median abundances too low (≤0.5%) to support robust interpretations. Both amplicon datasets were rarefied to avoid library size differences using phyloseq v.1.44 (McMurdie and Holmes 2013).

Chao1 and Shannon diversity metrics were estimated using phyloseq v.1.44, and the individual and combined effects of hydrothermal treatment and environmental conditions on species

alpha diversity were analysed through two-way ANOVA with rstatix v.0.7.2 (Kassambara 2021). An additional grouping variable called 'environmental conditions' was included in the analysis to account for seasonal differences in the initial sample. To assess the uncertainty in hierarchical clustering based on Bray–Curtis dissimilarities, multiscale bootstrap resampling was performed using pvclust v2.2 (Suzuki, Terada, and Shimodaira 2019) to obtain unbiased probabilities (au) for each cluster, which were later plotted with ggtree v3.8.2 (Yu 2020). PERMANOVA tests were then conducted to evaluate the relative contribution of hydrothermal treatment and environmental conditions, along with their interaction, to prokaryotic and eukaryotic community structure using vegan v2.6.4 (Oksanen et al. 2019). Additionally, indicator species analyses were computed using indicspecies v1.7.12 (De Cáceres and Legendre 2009) to identify microbial species most strongly associated with hydrothermally enriched environments, based on their occurrence and abundance in the treated incubations. We only considered those phylotypes most often found in surface waters affected by hydrothermal emissions, with an indicator value greater than 85% ($stat > 0.85$), a statistical significance $p \leq 0.001$ and mostly absent from controls ($str_C \leq 0.5$). All analyses were computed in R v4.3.1 (R Core Team 2021) and processed using tidyverse v2.0 (Wickham et al. 2019).

3 | Results

3.1 | Physical–Chemical Characterisation of Vent Fluids and Waters Affected by Tagoro

Seawater above the primary crater of Tagoro submarine volcano exhibited higher temperatures, increased acidity and greater $Si(OH)_4$ concentrations, as compared to unaffected seawater (Table S2). Thermal anomalies were larger in autumn (+0.37°C) than in spring (+0.09°C), whereas a consistent pH anomaly of −0.1 was observed across seasons. $Si(OH)_4$ concentrations ranged from 2.67 to 5.84 μmol kg^{-1}, reflecting a 3–6-fold increase compared to unaffected seawaters, with maximum concentrations observed in spring. Vent fluids were ~9°C warmer than the water column and exhibited the highest concentrations of dissolved inorganic nutrients, particularly $Si(OH)_4$ at 18.3 ± 1.2 μmol kg^{-1} and PO_4^{3-} at 15.6 ± 4.8 μmol kg^{-1} (Table S2).

The MLD south of El Hierro showed seasonal variations (Figure 3). Median MLD estimates were deepest in spring, reaching depths of ~121 m, followed by winter at ~96 m, and autumn at ~70 m. MLD estimates varied largely as expected; however, the mixed layer often extended below the summit of Tagoro (≥ 89 m depth) throughout the year and occasionally below its primary crater (≥ 127 m), particularly in spring and winter (Figure 3). Nevertheless, mixing events deeper than the primary crater also occurred in autumn.

3.2 | Dissolved Inorganic and Organic Compounds Throughout the Incubations

The treatment strategy resulted in proportional enrichments of $Si(OH)_4$ in the treated bottles, ranging from 0.9 to 2 μmol kg^{-1} (Figure 4A). No measurable changes were observed in the concentration of $NO_2^- + NO_3^-$ and PO_4^{3-} following the enrichment (Figure 4A). Both the hydrothermally enriched seawater and the vent fluids had concentrations in the lower range of the concentrations measured in previous studies. Thus, instead of the 4–16-fold nutrient enrichment expected, our initial conditions corresponded to a range between 0.97- and 1.83-fold enrichment in $Si(OH)_4$. These additions mimicked mixing conditions observed between 41 and 95 m away from the primary crater of Tagoro (Figure 4B). Since $Si(OH)_4$ concentrations were higher in the spring experiments, in this season the volcano-treated bottles corresponded to those observed at distances ranging from 41 to 63 m from the active sources of hydrothermal activity in Tagoro. In autumn, the volcano-treated bottles represented more distant waters, about 67–88 m. The vent-treated bottles resulted in the lowest hydrothermal additions, with $Si(OH)_4$ concentrations corresponding to about 95 m. The concentrations of dissolved inorganic nutrients were nearly depleted by the end of all treated incubations. Conversely, DOC and DON concentrations increased in the volcano-treated bottles, whereas they slightly decreased in the vent-treated bottles (Table S3).

3.3 | Microbial Growth

Regardless of the season, hydrothermal additions led to higher phytoplankton biomass (assessed through chlorophyll *a* concentration) and faster apparent growth rates compared to controls (Figure 5). Phytoplankton biomass in the volcano-treated bottles peaked at 2.5–7.8 μg Chl *a* L^{-1} after 5–7 days of incubation, occurring a day earlier than in the controls. Afterwards, a gradual decrease in biomass was observed until the end of the incubations. The vent-treated bottles, on the other hand, required an additional 2 days to achieve phytoplankton biomasses between 2.0 and 2.8 μg Chl *a* L^{-1}.

Flow cytometric analyses (Figures S2 and S3) showed that picoeukaryotes and *Synechococcus* populations (0.2–2 μm) benefited from hydrothermal enrichments. The cell abundance of picoeukaryotes increased exponentially in both volcano-treated and control bottles until Days 5 and 6 (Figures S2A and S3A). Despite the obvious differences between the autumn and spring samples, picoeukaryotes reached their maximum abundance earlier in the hydrothermally enriched treatments as compared to the corresponding controls. *Synechococcus* populations also exhibited earlier and faster increases in cell abundances in the presence of hydrothermal products (Figures S2B and S3B), with maximum values 3-fold higher than the controls. Interestingly, *Synechococcus* continued exponential growth in the controls after the collapse of their treated counterparts during the spring incubations, suggesting a top-down control in the volcano-treated bottles that did not happen in the controls. Although differences between control and vent-treated bottles were small for both populations (Figure S3A,B), Incubations 3 and 4 displayed *Synechococcus* abundances that were 3- to 4-fold higher 6 days after the vent enrichment, and these populations predominated thereafter. In contrast, *Prochlorococcus* populations grew regardless of the treatment throughout all incubations, although usually reached higher final cell abundances in treated bottles than in controls (Figures S2C and S3C). Heterotrophic bacteria showed little difference in cell abundances between treated

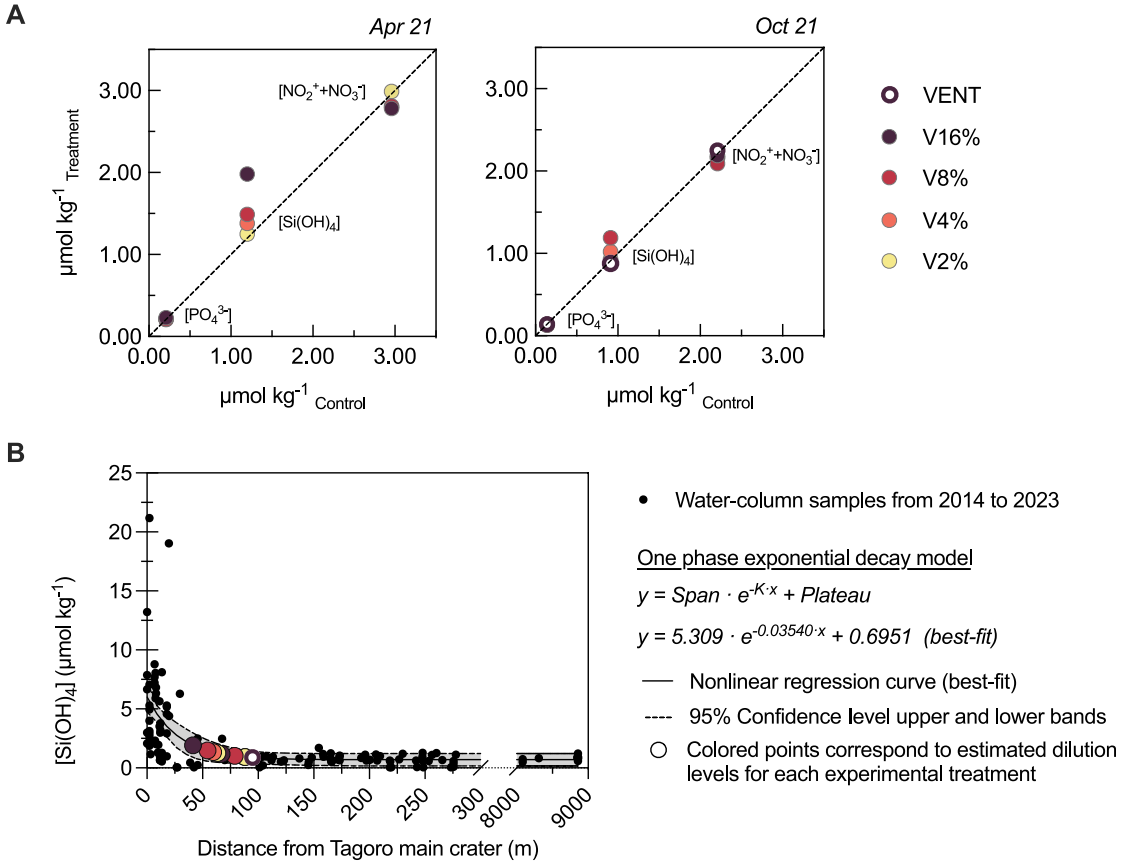

FIGURE 4 | (A) Initial dissolved inorganic nutrient concentrations (µmol kg^{-1}) in control versus volcano- and vent-treated bottles in April and October 2021 experiments. Data are also reported in Table S3. (B) Exponential decay fitting of dissolved inorganic silicate (µmol kg^{-1}) versus distance from the main crater of Tagoro (m), based on a decade of in situ measurements at seawater depths of 120–130 m. The exponential decay equation, 95% confidence intervals and estimated dilution levels (distance to the main crater) for each experimental treatment (see Section 2.2).

bottles and controls, even though some stimulation of growth was detectable in all cases after the collapse of the phytoplankton populations (Figure S4).

In addition, molecular analyses revealed that all treated bottles were primarily composed of small photosynthetic eukaryotes (≤5 µm) belonging to the divisions Dinoflagellata (dinoflagellates), Ochrophyta (photosynthetic stramenopiles), Chlorophyta (small green algae) and Radiolaria (protists) (Figure 6), rather than Cyanobacteria, which accounted for a low proportion of sequences (≤1%) in most cases (Figure 7). The initial eukaryotic and prokaryotic microbial communities in our incubations were similar to those found in situ in seawater adjacent to the primary active sources of Tagoro (Figure S5), including the photo- and chemoautotrophic organisms later found in the incubations.

Dinoflagellates were the prevailing group in the treated bottles as opposed to the controls, often accounting for half of the eukaryotic community at the end of the incubations (Figure 6). The class Syndiniales dominated with median relative abundances of 42% in the treated bottles (Figure 6A) and was mostly composed of parasitic dinoflagellates (Figure 6B), including Dino-Group I Clades 1 and 4 (> 10%) and Dino-Group II Clades 10 and 11 (2%–3%). A total of 24 ASVs belonging to these families were indeed significantly associated with the hydrothermal additions according to the indicator species analyses ($stat \geq 0.85$, $p \leq 0.001$ and $str_C \leq 0.4$; Table S4), comprising 19% of the relative abundance of species (Figure S6). Regarding the Dinophyceae class, it comprised about 5%–7% of Dinoflagellata at the end of the treated incubations (Figure 6A), with approximately 2% of the sequences belonging to the Gymnodiniaceae family (Figure 6B). However, it was a member of the Blastodiniaceae family (≤1%) that showed a significant association with the treatment ($stat = 0.95$, $p \leq 0.001$ and $str_C = 0.14$; Table S4), being the only one among the Dinophyceae class.

Meanwhile, photosynthetic stramenopiles were the second most abundant division throughout the treated incubations (Figure 6). Although their relative abundances increased 2-fold higher in control bottles, where they ended up comprising half of the eukaryotic community, the stramenopile assemblage was generally composed of diatoms (Bacillariophyta, 17%–33% of relative abundance) and other heterokonts (Pelagophyceae, 4%–12%) in all incubations (Figure 6A). Diatoms were primarily composed of polar centric Mediophyceae diatoms (16%–24%), which included a diverse range of low-abundance diatoms, and to a lesser extent, raphid pennate diatoms (3%–10%) (Figure 6B). Despite these observations, the pico- and nano-sized (2–20 µm) planktonic polar-centric species *Chaetoceros tenuissimus*, *Arcocellulus cornucervis* and *Minutocellus polymorphus* showed significant associations with the treated bottles ($stat \geq 0.91$, $p \leq 0.001$ and $str_C \leq 0.3$; Table S4), even though most of them

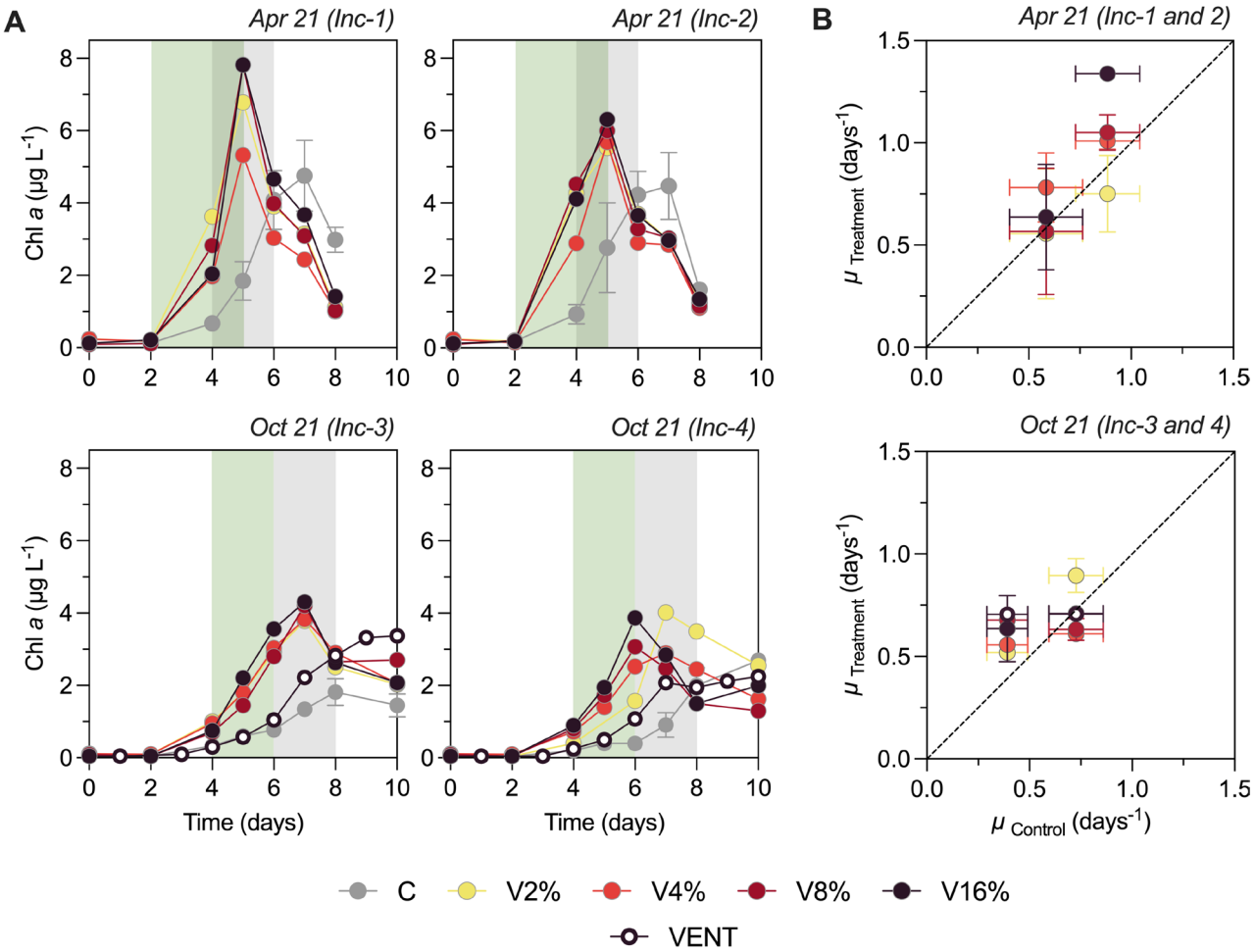

FIGURE 5 | (A) Chlorophyll *a* concentration (µg Chl *a* L^{-1}) in April and October 2021 incubations. Control (grey) dots represent the average and standard deviation from two replicate control bottles placed in each incubator (Inc). In contrast, volcano- (colour gradient) and vent-treated (white) dots represent individual bottles, each enriched with a proportion of filtered hydrothermal seawater (ranging from 2% to 16% of the total volume) or with 2% of vent fluids. Shaded areas indicate the exponential growth phase in control (grey) versus volcano- and vent-treated (green) bottles. (B) Apparent phytoplankton growth rates ($days^{-1}$) estimated from the exponential growth phases.

exhibited abundances below 1% (Figure S6). Pelagomonadaceae (4%–12%) predominated among Pelagophyceae at the end of all incubations (Figure 6B), and especially those identified as *Pelagomonas* (4%–9%), with *Pelagomonas calceolata* (3.5%–9%) as the primary species. However, only one ASV within this family could be significantly associated with the hydrothermal treatment ($stat = 0.91$, $p \leq 0.001$ and $str_C = 0.3$; Table S4).

Small green algae were the third most abundant division at the end of all incubations, even though they appeared to be the most enriched by the hydrothermal treatments (19%–21% of relative abundance), generally doubling the increases observed in control bottles (Figure 6). The family Chloropicaceae, belonging to the Chloropicophyceae class, particularly benefited from the treatments (Figure 6B), holding median relative abundances up to 9% at the end of the volcano- and vent-treated bottles. Since it was majorly composed of *Chloropicon* (~9%) and a few *Chloroparvula* (<1%), the indicator species analyses pointed to *Chloropicon roscoffensis* as the species most closely related to the hydrothermal treatments ($stat \geq 0.87$, $p \leq 0.001$ and $str_C \leq 0.4$; Table S4). A total of 10 ASVs of *C. roscoffensis* were, in fact, significantly associated with the treated incubations, accounting for 12% of the relative abundance at the end (Figure S6). Other classes of Chlorophyta also had higher relative abundances compared to controls, such as Trebouxiophyceae, Prasino Clade V and Mamiellophyceae (Figure 6A), yet exhibited median relative abundances below 3%.

Lastly, analyses showed that the Radiolaria division was enriched, with low relative abundances (1%–2%) and primarily composed of RAD-A protozoa, in the bottles treated with hydrothermal products (Figure 6).

These differences in the taxonomic composition of the eukaryotic community between controls and treatments were also evidenced by hierarchical clustering analyses, as replicate control bottles clustered together and apart from treated bottles with high bootstrap probabilities (Figure 6). Treatment accounted for 28% of the variance in eukaryotic composition recorded at the end of the experimental period (df = 1, $r^2 = 0.277$; $F = 10.4$, $p < 0.001$, PERMANOVA), whereas about 24% was explained by the environmental conditions (i.e., minor variations related to seasonal differences in the initial sample) (df = 3, $r^2 = 0.245$; $F = 3.07$, $p < 0.01$, PERMANOVA test). Fewer significant differences were observed in the composition of the prokaryotic community relative to the treatment (Figure 7), consistent with the small differences

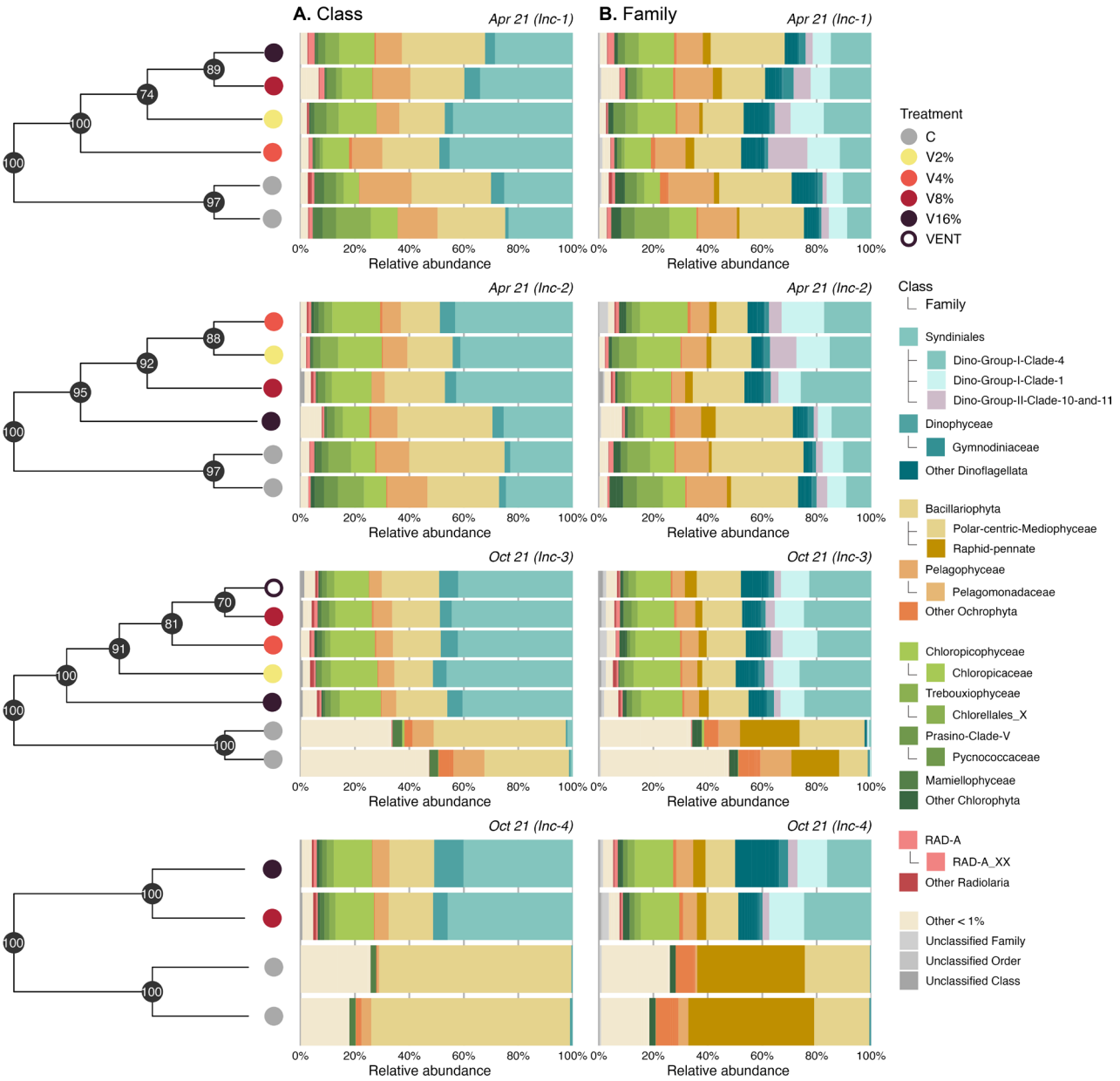

FIGURE 6 | Hierarchical clustering and relative abundance of eukaryotic 18S rRNA sequences classified down to (A) class and (B) family level for each incubation (Inc). Coloured dots represent the control (grey), volcano-treated (colour gradient) and vent-treated (white) bottles at the end of the April and October 2021 incubations. Volcano bottles were enriched with filtered hydrothermal seawater at concentrations ranging from 2% to 16% of the total volume, whereas vent bottles were treated with a 2% addition of vent fluids. Black points in the dendrogram represent the approximately unbiased *p* value (au) for each cluster. Taxa are ordered by decreasing relative abundance greater than 1% and grouped by the highest division groups.

observed in heterotrophic bacterial cell abundances (Figure S4). Nonetheless, the treatment was responsible for 20% of the prokaryotic variance (df = 1, $r^2 = 0.201$; $F = 13.18$, $p < 0.001$, PERMANOVA test), whereas environmental conditions explained 39% of the variance (df = 3, $r^2 = 0.386$; $F = 8.45$, $p < 0.001$, PERMANOVA test).

Regarding the prokaryotic community composition, most treated bottles consisted of the phyla Proteobacteria, Bacteroidota and Actinobacteriota, followed by Crenarchaeota (Figure 7).

Proteobacteria (67%–75%) was the most abundant phylum, comprising the classes Alphaproteobacteria (40%–46%) and Gammaproteobacteria (25%–28%). The Proteobacteria displayed some differences between control and treated bottles at the end of the incubations (Figure 7A) and contained the majority of the ASVs associated with the hydrothermal treatments (Table S5). Rhodobacteraceae (18%), Clade I (6%–8%), AEGEAN-169 marine group (3%–3.5%) and Clade II (2.5%–3.5%) families of Alphaproteobacteria predominated throughout the volcano- and vent-treated bottles (Figure 7B). Additionally, Hyphomonadaceae (2.5%–3%) and SAR116 clade (2.5%–3%) were some of the most benefited by the addition of hydrothermal products. A total of 31 alphaproteobacterial ASVs were associated with the treated bottles ($stat > 0.85$, $p \leq 0.001$ and $str_C \leq 0.5$; Table S5). Among these, many classified as SAR116 clade, AEGEAN-169 marine group, Clade II and Rhodobacteraceae stood out in terms of relative abundance (≤2%) (Figure S7). The diverse clade SAR86 (Gammaproteobacteria) was also

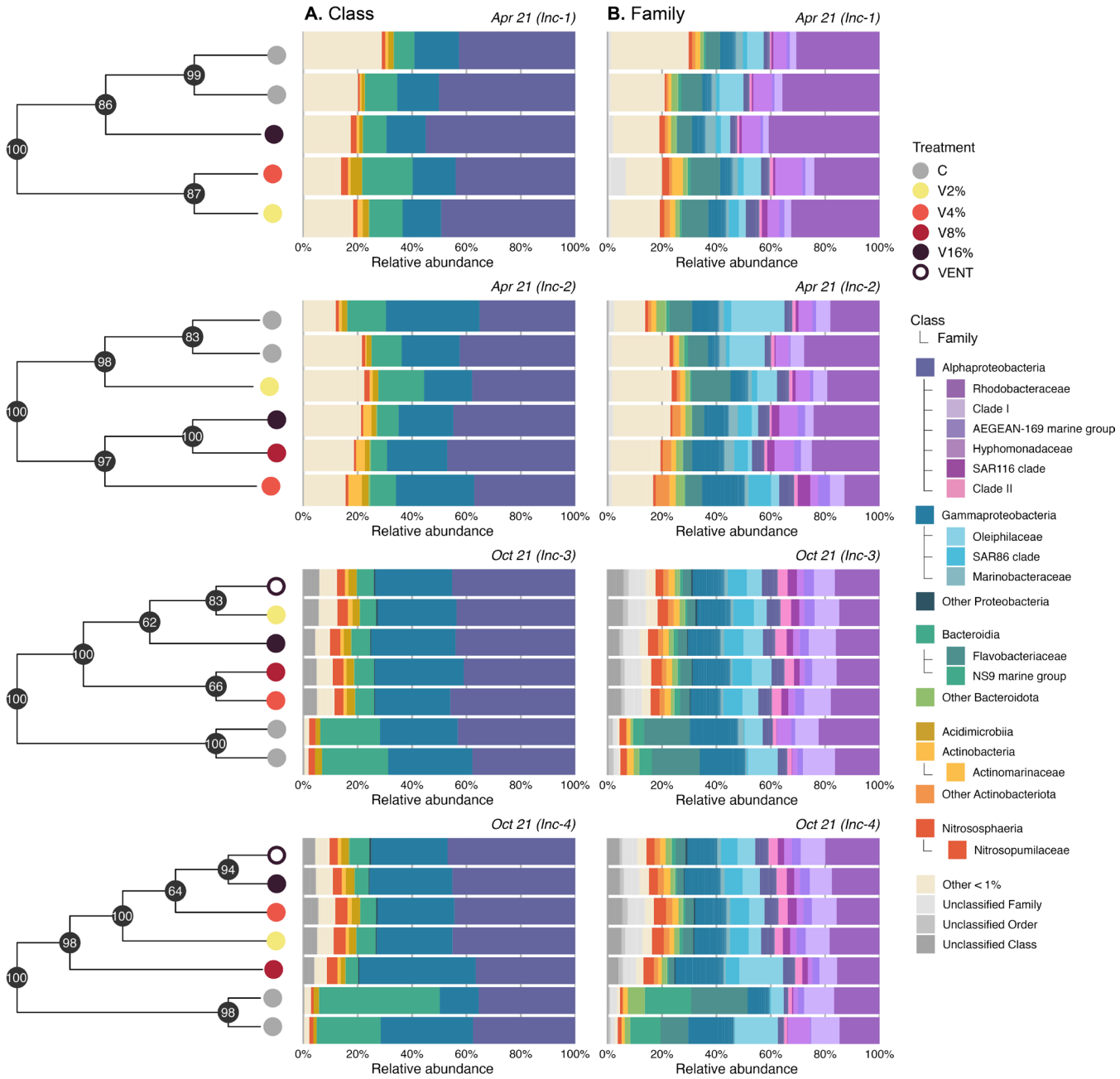

FIGURE 7 | Hierarchical clustering and relative abundance of prokaryotic 16S rRNA sequences classified down to (A) class and (B) family level for each incubation (Inc). Coloured dots represent the control (grey), volcano (colour gradient) and vent-treated (white) bottles at the end of the April and October 2021 incubations. Volcano bottles were enriched with filtered hydrothermal seawater at concentrations ranging from 2% to 16% of the total volume, whereas vent bottles were treated with a 2% addition of vent fluids. Black points in the dendrogram represent the approximately unbiased *p* value (au) for each cluster. Taxa are ordered by decreasing relative abundance greater than 1% and grouped by the highest phylum groups.

favoured by the additions (6.5%–7%) and contributed 14 out of 40 gammaproteobacterial ASVs (≤4%) indicative of hydrothermal treatment ($stat > 0.85$, $p \leq 0.001$ and $str_C < 0.5$; Table S5 and Figure S7). The remaining ASVs included several genera of phototrophic and chemotrophic Gammaproteobacteria, each below <1% (Table S5 and Figure S7), such as *Litoricola*, *Pseudomonas*, the *OM60 (NOR5) clade*, the *SUP05 cluster* and *Pseudoalteromonas*.

Indicator species analyses identified another 25 ASVs, belonging to the phyla Actinobacteriota, Bacteroidota, Firmicutes, Desulfobacterota and Marinimicrobia (SAR406 clade), as treatment indicators ($stat > 0.85$, $p \leq 0.001$ and $str_C < 0.5$; Table S5). This group included around 14 genera and 9 species of low-abundance (≤0.5%) bacteria (Table S5), such as the free-living photoheterotrophs *Candidatus* Actinomarina (Actinobacteriota) and *NS5 marine group* (Bacteroidota), the chemoorganotrophic *Fabibacter* (Bacteroidota) and several human pathogens.

Lastly, the Crenarchaeota archaeal lineage was exclusively composed of the chemolithoautotrophic ammonia oxidisers Nitrosopumilaceae in all incubations (Figure 7). Despite a consistent decrease in their abundance across all treatments, their

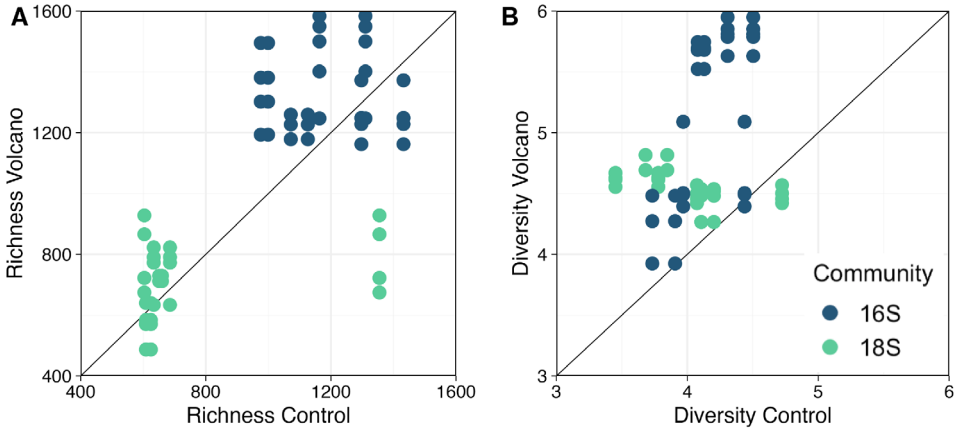

FIGURE 8 | Control versus volcano and vent-treated (A) Chao1 richness and (B) Shannon diversity estimates at the end of the incubations. Volcano bottles were enriched with filtered hydrothermal seawater at concentrations ranging from 2% to 16% of the total volume, whereas vent bottles were treated with a 2% addition of vent fluids.

final relative abundances were higher in the treated bottles (~3%) than in the controls (~1%).

The treated bottles exhibited the largest prokaryotic richness and diversity of ASVs (Figure 8A,B). Statistical analyses identified the hydrothermal treatment as the primary factor significantly influencing prokaryotic alpha diversity ($p < 0.01$, two-way ANOVA), followed by other factors related to the environmental conditions (including seasonal variations) ($p < 0.05$, two-way ANOVA). Meanwhile, the number of eukaryotic ASVs (richness) at the end of the treated incubations was generally higher relative to controls (Figure 8A), but exhibited some variability primarily influenced by the environmental conditions ($p < 0.05$, two-way ANOVA) rather than the treatment ($p > 0.05$, two-way ANOVA). In contrast, eukaryotic diversity was significantly modulated by the treatment ($p \leq 0.001$, two-way ANOVA), with hydrothermally enriched waters displaying higher diversity estimates compared to controls (Figure 8B). Moreover, the alpha diversity estimates of prokaryotes at the end of the treated incubations surpassed those of eukaryotes (Figure 8A,B).

4 | Discussion

Shallow-water hydrothermal vents constitute unique ecosystems rich in nutrients and reduced compounds, where primary production is often sustained by both photosynthesis and chemosynthesis (e.g., Tarasov et al. 2005; Maugeri et al. 2010). Using an experimental approach, we assessed for the first time the effects of diffusive hydrothermal emissions on microbial community abundance, structure and diversity at the Tagoro shallow submarine volcano in El Hierro (Canary Islands, Spain).

4.1 | Effects of Shallow Hydrothermal Fluids on the Growth of Marine Microbes

Phytoplankton biomass and growth estimates, assessed by means of chlorophyll *a* concentration, exhibited the greatest increases in the volcano-treated bottles. Although the vent-treated bottles received the lowest hydrothermal enrichment, as indicated by $Si(OH)_4$ concentrations, they still exceeded control estimates. However, the increase in phytoplankton biomass in the vent-treated bottles was observed 2 days later than those in the volcano-treated bottles, possibly due to the small amount of nutrients added and/or the presence of toxic constituents that may have affected phytoplankton growth. These findings clearly show that hydrothermal fluids from Tagoro stimulate phytoplankton growth in shallow waters (i.e., primary production), inducing a fertilisation effect that may be detectable even up to a 100 m away from the active source and despite seasonal variations. This is consistent with in situ and experimental evidence across hydrothermal systems worldwide, where inorganic nutrients such as bioavailable Fe provided by hydrothermal inputs enhance primary productivity in the surface layer (e.g., Buck et al. 2018; Guieu et al. 2018; Bonnet et al. 2023; Tilliette et al. 2023). In a similar experiment carried out in the Western Tropical South Pacific Ocean, Tilliette et al. (2023) observed a clear stimulation of net community production following the addition of hydrothermal fluids to indigenous phytoplankton communities.

The enhancement in phytoplankton biomass likely led to high dissolved organic matter production in our treated incubations, thereby driving microbial utilisation of organic material. Besides introducing trace metals like Fe that serve as micronutrients for plankton communities (Guieu et al. 2018; Ardyna et al. 2019; Schine et al. 2021; Bonnet et al. 2023; Mériguet et al. 2023), hydrothermal fluids also contain essential metals that may become harmful at the high concentrations found near vents (e.g., Cu and As) (Lilley, Feely, and Trefry 1995; Price et al. 2013). In this context, vent microorganisms have been shown to produce organic ligands to either enhance the bioavailability of some essential metals or decrease their toxicity at high levels (Klevenz et al. 2012). Recently, some *Synechococcus* ecotypes have been observed to produce strong binding ligands, especially thiols, proving their ability to detoxify the environment and thus favour phytoplankton growth (Tilliette et al. 2023). These findings raise concerns about the potential impact of toxic metals on plankton communities near Tagoro and suggest that common surface microbes may possess mechanisms to overcome these extreme conditions. Despite the absence of direct measurements, significant amounts of heavy metals have been observed in cephalopods captured in the vicinity of this submarine

volcano (Lozano-Bilbao et al. 2022), supporting the idea that vent fluids from Tagoro contain relevant concentrations of toxic elements. However, both auto- and heterotrophic microbes grew equally well or better in the presence of hydrothermal fluids as compared to controls. This indicates that, even if some toxic metals may have been present, their effect on productivity was small as compared to the stimulation caused by the other components of hydrothermal fluids.

The stimulation of primary production in the incubations enriched with hydrothermal fluids was coupled with increases in cell abundances of certain photosynthetic picoplankton (0.2–2 μm) populations. Picoeukaryotes and *Synechococcus* picocyanobacteria reached cell abundances that were 3- to 5-fold higher than those in controls, evidencing their ability to thrive in hydrothermally enriched habitats. Despite the lower hydrothermal enrichment in the vent-treated bottles, some *Synechococcus* populations managed to increase their cell abundances up to 4-fold higher than in controls. *Prochlorococcus* picocyanobacteria and heterotrophic bacteria, on the other hand, grew similarly well across all treatments, albeit they reached higher cell abundances in the presence of hydrothermal fluids. Other experimental studies have shown similar results, where picocyanobacterial growth (mainly *Synechococcus*) was sustained by dissolved Fe concentrations provided by hydrothermal inputs (Tilliette et al. 2023).

Molecular analyses further revealed a strong presence of small photosynthetic eukaryotes (≤5 μm) in the treated bottles, including dinoflagellates, photosynthetic stramenopiles, small green algae and radiolarians, which likely supported the enhancement in chlorophyll *a* levels. The treated bottles also supported the growth of ecologically and metabolically diverse prokaryotes, comprising chemosynthetic and photosynthetic bacteria, as well as a few ammonia-oxidising archaea. It is relevant to emphasise that, despite the enhancement of phytoplankton growth, hydrothermal inputs from Tagoro did not result in harmful, disruptive events such as the proliferation of harmful algal species. Instead, they sustained the enhanced growth of many microbial populations already present in the area, as discussed in Section 4.2. Remarkably, the natural communities collected at a depth of 127 m, both around the crater and in unaffected waters, already contained a large proportion of the photoautotrophic microbes that benefited from hydrothermal fluid additions. This indicates that enhanced photosynthesis may occur not only when hydrothermal fluids mix with surface waters but also in deeper waters around the main crater. Our estimates of the MLD and in situ dissolved silicate concentrations further confirm that, especially in spring, hydrothermal, nutrient-rich products often reach photosynthetic organisms near the Tagoro submarine volcano, a scenario we aimed to replicate in our experiments.

4.2 | Effects of Shallow Hydrothermal Fluids on the Composition and Diversity of Marine Microbes

The taxonomic composition of the eukaryotic community differed between controls and treated bottles, with volcano- and vent-treated bottles developing characteristic communities, as evidenced by hierarchical clustering analyses. Statistical analyses further indicated that, despite variations in environmental conditions (i.e., seasonal or minor variations in physical–chemical properties of the water column), hydrothermal inputs from the Tagoro submarine volcano induced a clear response in the eukaryotic community structure.

Photosynthetic stramenopiles, primarily comprising diatoms (Bacillariophyta), along with other heterokonts (Pelagophyceae), exhibited a significant presence across all incubations. However, their relative abundance was twice as high in the control samples compared to the treated bottles, and they consistently maintained the second highest representation within the treated incubations. Among the predominant and varied diatom community, the less abundant (≤1%) pico- and nanoplanktonic polar-centric species, including *C. tenuissimus*, *A. cornucervis* and *M. polymorphus*, demonstrated a robust association with hydrothermal inputs, as they were predominantly observed in treated bottles. Diatoms, unlike other major phytoplankton groups, strictly depend on dissolved silicon, along with sufficient light, inorganic nutrients and trace elements, to sustain their fast growth rates (Morel and Price 2003). Although the surface waters affected by Tagoro may provide favourable conditions for diatom proliferation, as evidenced by nutrient depletion at the end of the treated incubations, our findings suggest that factors such as resource competition, selective grazing and viral activity may control the extent of their response. Centric diatoms in the planktonic realm have the ability to adjust their buoyancy, allowing them to move vertically within the water column. This capability may provide these species with advantages in resource competition and predator evasion (Armbrust 2009). Our findings emphasise the ability of certain diatom species to benefit from changing ambient conditions and thus contribute to the overall productivity of the system (Benoiston et al. 2017; Serôdio and Lavaud 2020). Recent evidence has demonstrated that the small pico- and nanoplanktonic diatom cells, often overlooked, may not only fuel the microbial loop but also contribute to sustaining higher trophic levels and facilitating carbon export (Leblanc et al. 2018). Therefore, small planktonic diatoms (mostly centric forms) may exert a significant impact on the productivity, nutrient cycling and carbon sequestration in Tagoro. Other high-abundance heterokont species, such as *P. calceolata*, were largely unaffected by the addition of hydrothermal fluids. The persistence of this specific species throughout the incubations underscored its adaptative capacities, as *P. calceolata* is known to thrive under the high temperature, low light and low iron conditions (Guérin et al. 2022) typical of the deep, unaffected waters at the sampling location. These traits might explain its low diversity compared to that of diatoms in the context of a shallow hydrothermal system characterised by $Si(OH)_4$, $NO_2^- + NO_3^-$, and presumably Fe-rich seawaters, which are quite different from those conditions where *Pelagomonas* may be a strong competitor.

Small green algae emerged as a key contributor to local primary production, doubling the increases in relative abundances observed in controls. The hydrothermal additions notably benefited the Chloropicophyceae prasinophyte lineage, particularly the Chloropicaceae family. The Prasino Clade V and Mamiellophyceae prasinophyte lineages, together with the

Trebouxiophyceae class (core Chlorophyta), also exhibited higher relative abundances compared to controls. These independent prasinophyte lineages comprise small-sized coccoid species that play a key role in marine phytoplankton communities, especially in moderately oligotrophic waters (Lopes dos Santos et al. 2017). Their higher surface area-to-volume ratio enhances nutrient uptake efficiency and thus improves their competitiveness in nutrient-poor environments, facilitates their escape from predators and promotes buoyancy (Lemieux et al. 2019). These traits may grant Chloropicophyceae, and particularly the species *C. roscoffensis*, with the necessary advantages to outcompete other planktonic algae under the moderate nutrient concentrations in our hydrothermal additions. *Chloropicon* presence is ubiquitous across the globe, known for its ability to recycle propionate for carbon and energy sources, as well as synthesise scarce vitamins, among other traits (Lemieux et al. 2019). The indicator species analysis underscored the responsiveness of this particular species, with 10 ASVs identified as treatment indicators.

Our study also revealed the important role of protists, mostly dinoflagellates, in modulating the marine plankton dynamics within the Tagoro ecosystem. Contrary to the controls, dinoflagellates constituted half of the eukaryotic community at the end of the treated incubations. Syndiniales, a diverse group of unicellular parasites, emerged as the dominant class, with several families being linked to the presence of hydrothermal fluids, including Dino-Group I Clades 1 and 4, and Dino-Group II Clades 10 and 11. Interestingly, these groups are common inhabitants of deep sea hydrothermal vents (Hu et al. 2023), emphasising the importance of parasitic protists in the ecology of submarine hydrothermal vents. As already observed in deep sea hydrothermal vent ecosystems, the enhanced biological activity associated with diffusive vent fluids increases host and prey biomass and thereby parasitic encounters and infection. Syndiniales display putative parasite–host relationships with a wide range of hosts, such as other dinoflagellates and protist groups (e.g., ciliates, radiolarians, diatoms and copepods) (Anderson and Harvey 2020), yet these relationships remain poorly understood. Recent studies have shown that Syndiniales are often associated with Dinophyceae and Arthropoda (mainly copepods) in surface oligotrophic waters (Anderson et al. 2024). In our treated bottles, hydrothermal inputs indeed favoured the less abundant Dinophyceae class, with relatively large contributions of family Gymnodiniaceae, a recognised putative host of Syndiniales (Guillou et al. 2008). In addition, the less abundant species *Blastodinium mangini* within Dinophyceae exhibited a significant association with the treated bottles. *Blastodinium* is known to inhabit the gut of planktonic copepods, especially in warm temperate to tropical waters (Skovgaard, Karpov, and Guillou 2012), which aligns with previous observations of enhanced zooplankton growth in waters affected by degassing emissions at Tagoro (Fernández de Puelles et al. 2021). Indeed, those authors observed a significant presence of *Oncaea* non-calanoid copepods, which are frequently infected by *B. mangini* (Skovgaard, Karpov, and Guillou 2012). Mixotrophic protists like Radiolaria, known for their phagotrophic feeding (Biard 2022), also benefited from the presence of hydrothermal products in our incubations, despite their relatively low representation. Their prey includes bacteria, small autotrophs (like diatoms and dinoflagellates), other protists (mostly ciliates and tintinnids) and even multicellular heterotrophs (like copepods). These findings suggest an important top-down pressure exerted by protist marine phagotrophy and parasitism on the local plankton community at Tagoro. Protistan grazing thus not only represents an important ecological link in food webs by transferring organic carbon from primary producers to higher trophic levels (Hu et al. 2021) but also to the microbial loop (Park, Yih, and Coats 2004). Recent studies have indicated that Syndiniales in particular may contribute to attenuating the particulate carbon flux through remineralisation of host carbon that in the end may fuel bacterial production (Anderson et al. 2024). However, the contribution of parasitism to pools of dissolved organic matter in the ocean is uncertain. Contrarily, Radiolaria are active players in the biogeochemical cycles of silica, carbon and strontium, depending on their main skeletal chemical component (Biard 2022). These findings indicate that protistan activity will not only influence the planktonic community structure but also the local cycling of nutrients.

Alpha diversity estimates, encompassing richness and diversity, indicated the pronounced dominance of a select few eukaryotic populations within the overall assemblage observed in the treated bottles. This finding, supported by robust statistical significance, highlights a marked specialisation within the eukaryotic community in response to the hydrothermally enriched conditions, in contrast to the prokaryotic community.

Conversely, the differences in prokaryotic community structure between control and treated bottles were mostly driven by the environmental conditions, such as seasonal variations in the properties of the water column. Although hydrothermal inputs did have a significant effect on shaping the prokaryotic community, their overall impact was minor. As mentioned in Section 4.1, a great diversity of ecologically and metabolically diverse prokaryotes was observed at the end of the treated incubations. Yet, the predominant Alphaproteobacteria and Gammaproteobacteria classes displayed some of the greatest differences throughout the incubations. Among the alphaproteobacterial ASVs significantly associated with the hydrothermal additions, the SAR116 clade, AEGEAN-169 marine group, Clade II and Rhodobacteraceae stood out in terms of relative abundance. Their presence in the treated bottles was likely related to their ability to utilise phytoplankton-derived organic matter and/or form symbiotic associations with marine eukaryotes to obtain carbon and other nutrients at hydrothermal vents. Moreover, many harbour distinct metabolic capacities that potentially allow them to adapt and thrive at particular habitat conditions, like those at hydrothermal vents. For instance, SAR116 have genes for proteorhodopsin-based photoheterotrophy, carbon monoxide dehydrogenase and dimethylsulfoniopropionate demethylase, which at the same time evidence the biogeochemical importance of this clade, especially in the marine sulfur cycle (Roda-Garcia et al. 2021). The AEGEAN-169 marine group, likewise, is known for its potential to transport and utilise a wide spectrum of sugars, trace metals and vitamins (Getz et al. 2023). Within the gammaproteobacteria, different ASVs belonging to the SAR86 clade were strongly linked to hydrothermal inputs. SAR86 is recognised as an aerobic chemoheterotroph with the potential for energy generation through proteorhodopsin (Dupont et al. 2012). Given its vast genetic diversity, distinct SAR86 subgroups have demonstrated a unique

geographic distribution closely associated with specific environmental characteristics (Hoarfrost et al. 2020), such as hydrothermal plumes (Zhou et al. 2020), consistent with our previous findings regarding other proteobacterial groups. Despite the clear dominance of Proteobacteria, several low-abundance bacteria species (≤0.5%) belonging to Actinobacteriota, Bacteroidota, Firmicutes, Desulfobacterota and Marinimicrobia (SAR406 clade) phyla were also identified as treatment indicators. Interestingly, members of Desulfobacterota appear as strong indicators of hydrothermal activity, indicating that sulfur oxidation may be an important microbial process in the water column around the Tagoro volcano. Moreover, the ubiquitous persistence of chemosynthetic microbes related to the oxidation of sulfur and ammonia throughout the treatments and controls highlights the potential for rapid dispersal of these organisms among different hydrothermal sites. Overall, our study indicates that the current hydrothermal fluids from Tagoro influence the prokaryotic community, directly by fueling chemosynthetic processes but also indirectly by supporting higher phototrophic production, as has been observed.

5 | Conclusion

Our findings confirm that hydrothermal processes affect surface microbial communities surrounding the Tagoro underwater volcano even a decade after its eruption. Phytoplankton biomass and growth increased in response to hydrothermal additions, demonstrating the potential of hydrothermal fluids to enhance primary production. This increase in primary production was accompanied by shifts in the structure and composition of the local marine microbial community, with notable contributions from small green algae (Chlorophyta) and diatoms (Bacillariophyta). Our analyses identified certain species within these groups as highly adapted to the new environmental conditions associated with the hydrothermal treatment. The results also indicated that parasitism by Syndiniales (Dinoflagellata) and protistan grazing may play a crucial role in modulating local plankton dynamics, ultimately shaping nutrient cycling and carbon export in the area. Phototrophic and chemotrophic bacteria also thrived in the treated bottles, although heterotrophic prokaryotes in the Tagoro hydrothermal ecosystem were the major drivers of prokaryotic growth. Overall, our findings support recent observations that shallow diffusive hydrothermal vent systems, such as the Tagoro submarine volcano, may enhance primary production rates locally by both phototrophic and chemoautotrophic processes. Our study demonstrates that shallow hydrothermal fluxes can serve as local drivers of microbial productivity, an aspect previously overlooked, highlighting the need for further research in this area.

Author Contributions

Clàudia Pérez-Barrancos: conceptualization, data curation, investigation, writing – original draft, methodology, visualization, writing – review and editing, software, formal analysis. **Eugenio Fraile-Nuez:** conceptualization, investigation, funding acquisition, writing – review and editing, methodology, resources, project administration, supervision, data curation. **Juan Pablo Martín-Díaz:** investigation, writing – review and editing. **Alba González-Vega:** investigation, writing – review and editing. **José Escánez-Pérez:** investigation, writing – review and editing. **María Isabel Díaz-Durán:** investigation, writing – review and editing. **Carmen Presas-Navarro:** investigation, writing – review and editing, project administration. **Mar Nieto-Cid:** supervision, writing – review and editing, resources. **Jesús María Arrieta:** conceptualization, investigation, funding acquisition, writing – original draft, methodology, validation, writing – review and editing, project administration, supervision, resources, data curation.

Acknowledgements

This research was supported by the projects POSEIDON (CTM2017-84735-R) and FAMOUS (PID2021-125368NB-I00) funded by MCIN/AEI, and by the Spanish Institute of Oceanography through project VULCANA-III (IEO-2021-2023). C.P.-B. was supported by a predoctoral grant (PRE2018-083800) funded by MCIN/AEI. We would like to thank the officers and crew of the R/V *Ángeles Alvariño* from the Spanish Institute of Oceanography and the technical team of ACSM (ROV) for their help at sea. We would also like to acknowledge the work and support of the entire team of scientists and technicians involved in the research projects VULCANA and POSEIDON. Special thanks to Professor Javier Arístegui for his constructive review and comments that largely improved the quality of this manuscript. This research was funded by the Spanish Institute of Oceanography (IEO-CSIC) through VULCANA-II-III-IV (IEO-CSIC-2015-2026) projects and with special funding from the Ministry of Science and Innovation of the Spanish Government (20223PAL005). Additional support was provided by the Spanish National Plan for I+D projects POSEIDON (CTM2017-84735-R) and FAMOUS (PID2021-125368NB-I00). C.P.-B. (PRE2018-083800) was supported by the Spanish Ministry of Science and Innovation during the experimental development of this study.

Conflicts of Interest

The authors declare no conflicts of interest.

Data Availability Statement

The data that support the findings of this study are openly available in NCBI SRA at https://www.ncbi.nlm.nih.gov/sra, reference number PRJNA1098582.

References

Álvarez-Valero, A. M., O. Sánchez-Guillamón, I. Navarro, et al. 2023. "From Magma Source to Volcanic Sink Under Tagoro Volcano (El Hierro, Canary Islands): Petrologic, Geochemical and Physiographic Evolution of the 2011–2012 Submarine Eruption." In *El Hierro Island*, edited by P. J. González, 61–89. Springer International Publishing.

Aminot, A., and R. Kérouel. 2007. *Dosage Automatique des Nutriments Dans les Eaux Marines: Méthodes en Flux Continu*. Editions Quae.

Anderson, S. R., L. Blanco-Bercial, C. A. Carlson, and E. L. Harvey. 2024. "The Role of Syndiniales Parasites in Depth-Specific Networks and Carbon Flux in the Oligotrophic Ocean." *ISME Communications* 4, no. 1: ycae014. https://doi.org/10.1093/ismeco/ycae014.

Anderson, S. R., and E. L. Harvey. 2020. "Temporal Variability and Ecological Interactions of Parasitic Marine Syndiniales in Coastal Protist Communities." *mSphere* 5, no. 3: e00209-20. https://doi.org/10.1128/msphere.00209-20.

Apprill, A., S. McNally, R. Parsons, and L. Weber. 2015. "Minor Revision to V4 Region SSU rRNA 806R Gene Primer Greatly Increases Detection of SAR11 Bacterioplankton." *Aquatic Microbial Ecology* 75: 129–137.

Ardyna, M., L. Lacour, S. Sergi, et al. 2019. "Hydrothermal Vents Trigger Massive Phytoplankton Blooms in the Southern Ocean." *Nature Communications* 10: 2451.

Ariza, A., S. Kaartvedt, A. Røstad, et al. 2014. "The Submarine Volcano Eruption Off El Hierro Island: Effects on the Scattering Migrant Biota and the Evolution of the Pelagic Communities." *PLoS One* 9: e102354.

Armbrust, E. V. 2009. "The Life of Diatoms in the World's Oceans." *Nature* 459: 185–192.

Benoiston, A.-S., F. M. Ibarbalz, L. Bittner, et al. 2017. "The Evolution of Diatoms and Their Biogeochemical Functions." *Philosophical Transactions of the Royal Society, B: Biological Sciences* 372: 20160397.

Biard, T. 2022. "Diversity and Ecology of Radiolaria in Modern Oceans." *Environmental Microbiology* 24: 2179–2200.

Bonnet, S., C. Guieu, V. Taillandier, et al. 2023. "Natural Iron Fertilization by Shallow Hydrothermal Sources Fuels Diazotroph Blooms in the Ocean." *Science* 380: 812–817.

Buck, N. J., J. A. Resing, E. T. Baker, and J. E. Lupton. 2018. "Chemical Fluxes From a Recently Erupted Shallow Submarine Volcano on the Mariana Arc." *Geochemistry, Geophysics, Geosystems* 19: 1660–1673.

Callahan, B. J., P. J. McMurdie, M. J. Rosen, A. W. Han, A. J. A. Johnson, and S. P. Holmes. 2016. "DADA2: High-Resolution Sample Inference From Illumina Amplicon Data." *Nature Methods* 13: 581–583.

Caramanna, G., S. M. Sievert, and S. I. Bühring. 2021. "Submarine Shallow-Water Fluid Emissions and Their Geomicrobiological Imprint: A Global Overview." *Frontiers in Marine Science* 8: 727199. https://doi.org/10.3389/fmars.2021.727199.

Danovaro, R., M. Canals, M. Tangherlini, et al. 2017. "A Submarine Volcanic Eruption Leads to a Novel Microbial Habitat." *Nature Ecology & Evolution* 1: 1–9.

de Boyer Montégut, C., G. Madec, A. S. Fischer, A. Lazar, and D. Iudicone. 2004. "Mixed Layer Depth Over the Global Ocean: An Examination of Profile Data and a Profile-Based Climatology." *Journal of Geophysical Research, Oceans* 109: C12003.

De Cáceres, M., and P. Legendre. 2009. "Associations Between Species and Groups of Sites: Indices and Statistical Inference." *Ecology* 90: 3566–3574.

Dupont, C. L., D. B. Rusch, S. Yooseph, et al. 2012. "Genomic Insights to SAR86, an Abundant and Uncultivated Marine Bacterial Lineage." *ISME Journal* 6: 1186–1199.

Fernández de Puelles, M. L., M. Gazá, M. Cabanellas-Reboredo, et al. 2021. "Abundance and Structure of the Zooplankton Community During a Post-Eruptive Process: The Case of the Submarine Volcano Tagoro (El Hierro; Canary Islands), 2013–2018." *Frontiers in Marine Science* 8: 923.

Ferrera, I., J. Arístegui, J. M. González, M. F. Montero, E. Fraile-Nuez, and J. M. Gasol. 2015. "Transient Changes in Bacterioplankton Communities Induced by the Submarine Volcanic Eruption of El Hierro (Canary Islands)." *PLoS One* 10: e0118136.

Fraile-Nuez, E., M. González-Dávila, J. M. Santana-Casiano, et al. 2012. "The Submarine Volcano Eruption at the Island of El Hierro: Physical-Chemical Perturbation and Biological Response." *Scientific Reports* 2: 486.

Fraile-Nuez, E., J. M. Santana-Casiano, M. González-Dávila, et al. 2023. "Ten Years of Intense Physical–Chemical, Geological and Biological Monitoring Over the Tagoro Submarine Volcano Marine Ecosystem (Eruptive and Degassing Stages)." In *El Hierro Island*, edited by P. J. González. Springer International Publishing.

Fraile-Nuez, E., J. M. Santana-Casiano, M. González-Dávila, et al. 2018. "Cyclic Behavior Associated With the Degassing Process at the Shallow Submarine Volcano Tagoro, Canary Islands, Spain." *Geosciences* 8: 457.

Getz, E. W., V. C. Lanclos, C. Y. Kojima, et al. 2023. "The AEGEAN-169 Clade of Bacterioplankton Is Synonymous With SAR11 Subclade V (HIMB59) and Metabolically Distinct." *mSystems* 8: e00179-23.

Gómez-Letona, M., J. Arístegui, A. G. Ramos, M. F. Montero, and J. Coca. 2018. "Lack of Impact of the El Hierro (Canary Islands) Submarine Volcanic Eruption on the Local Phytoplankton Community." *Scientific Reports* 8: 4667.

González, F. J., B. Rincón-Tomás, L. Somoza, et al. 2020. "Low-Temperature, Shallow-Water Hydrothermal Vent Mineralization Following the Recent Submarine Eruption of Tagoro Volcano (El Hierro, Canary Islands)." *Marine Geology* 430: 106333.

González, P. J., ed. 2023. *El Hierro Island*. Springer International Publishing.

González-Vega, A., J. M. Arrieta, M. Santana-Casiano, et al. 2023. "Tagoro Submarine Volcano as a Natural Source of Significant Dissolved Inorganic Nutrients." In *El Hierro Island*, edited by P. J. González, 185–201. Springer International Publishing.

González-Vega, A., I. Callery, J. M. Arrieta, J. M. Santana-Casiano, J. F. Domínguez-Yanes, and E. Fraile-Nuez. 2022. "Severe Deoxygenation Event Caused by the 2011 Eruption of the Submarine Volcano Tagoro (El Hierro, Canary Islands)." *Frontiers in Marine Science* 9: 834691. https://doi.org/10.3389/fmars.2022.834691.

González-Vega, A., E. Fraile-Nuez, J. M. Santana-Casiano, et al. 2020. "Significant Release of Dissolved Inorganic Nutrients From the Shallow Submarine Volcano Tagoro (Canary Islands) Based on Seven-Year Monitoring." *Frontiers in Marine Science* 6: 829.

Guérin, N., M. Ciccarella, E. Flamant, et al. 2022. "Genomic Adaptation of the Picoeukaryote Pelagomonas Calceolata to Iron-Poor Oceans Revealed by a Chromosome-Scale Genome Sequence." *Communications Biology* 5: 1–14.

Guieu, C., S. Bonnet, A. Petrenko, et al. 2018. "Iron From a Submarine Source Impacts the Productive Layer of the Western Tropical South Pacific (WTSP)." *Scientific Reports* 8: 9075.

Guillou, L., D. Bachar, S. Audic, et al. 2013. "The Protist Ribosomal Reference Database (PR2): A Catalog of Unicellular Eukaryote Small Sub-Unit rRNA Sequences With Curated Taxonomy." *Nucleic Acids Research* 41: D597–D604.

Guillou, L., M. Viprey, A. Chambouvet, et al. 2008. "Widespread Occurrence and Genetic Diversity of Marine Parasitoids Belonging to Syndiniales (Alveolata)." *Environmental Microbiology* 10: 3349–3365.

Hoarfrost, A., S. Nayfach, J. Ladau, et al. 2020. "Global Ecotypes in the Ubiquitous Marine Clade SAR86." *ISME Journal* 14: 178–188.

Holm-Hansen, O., C. J. Lorenzen, R. W. Holmes, and J. D. H. Strickland. 1965. "Fluorometric Determination of Chlorophyll." *Journal of Conservation and Perennial Integrative Exploration of the Marine Environment* 30: 3–15.

Hu, S. K., E. L. Herrera, A. R. Smith, et al. 2021. "Protistan Grazing Impacts Microbial Communities and Carbon Cycling at Deep-Sea Hydrothermal Vents." *Proceedings of the National Academy of Sciences of the United States of America* 118: e2102674118.

Hu, S. K., A. R. Smith, R. E. Anderson, et al. 2023. "Globally-Distributed Microbial Eukaryotes Exhibit Endemism at Deep-Sea Hydrothermal Vents." *Molecular Ecology* 32: 6580–6598.

Kassambara, A. 2021. "rstatix: Pipe-Friendly Framework for Basic Statistical Tests." R Package Version 0.7.0.

Klevenz, V., S. G. Sander, M. Perner, and A. Koschinsky. 2012. "Amelioration of Free Copper by Hydrothermal Vent Microbes as a Response to High Copper Concentrations." *Chemistry and Ecology* 28: 405–420.

Leblanc, K., B. Quéguiner, F. Diaz, et al. 2018. "Nanoplanktonic Diatoms Are Globally Overlooked but Play a Role in Spring Blooms and Carbon Export." *Nature Communications* 9: 953.

Lemieux, C., M. Turmel, C. Otis, and J.-F. Pombert. 2019. "A Streamlined and Predominantly Diploid Genome in the Tiny Marine Green Alga Chloropicon Primus." *Nature Communications* 10: 4061.

Lilley, M. D., R. A. Feely, and J. H. Trefry. 1995. "Chemical and Biochemical Transformations in Hydrothermal Plumes." In *Seafloor Hydrothermal Systems: Physical, Chemical, Biological, and Geological*

Interactions, edited by E. Humphris, R. A. Zierenberg, L. S. Mullineaux, and R. E. Thomsom, 369–391. American Geophysical Union (AGU).

LopesdosSantos, A., T. Pollina, P. Gourvil, et al. 2017. "Chloropicophyceae, A New Class of Picophytoplanktonic Prasinophytes." *Scientific Reports* 7: 14019.

Lorbacher, K., D. Dommenget, P. P. Niiler, and A. Köhl. 2006. "Ocean Mixed Layer Depth: A Subsurface Proxy of Ocean-Atmosphere Variability." *Journal of Geophysical Research, Oceans* 111: C07010.

Lozano-Bilbao, E., G. Lozano, Á. J. Gutiérrez, et al. 2022. "The Influence of the Degassing Phase of the Tagoro Submarine Volcano (Canary Islands) on the Metal Content of Three Species of Cephalopods." *Marine Pollution Bulletin* 182: 113964.

Marie, D., F. Partensky, S. Jacquet, and D. Vaulot. 1997. "Enumeration and Cell Cycle Analysis of Natural Populations of Marine Picoplankton by Flow Cytometry Using the Nucleic Acid Stain SYBR Green I." *Applied and Environmental Microbiology* 63: 186–193.

Martín-Díaz, J. P., A. González-Vega, T. Barreyre, et al. 2024. "Unveiling the Inherent Physical-Chemical Dynamics: Direct Measurements of Hydrothermal Fluid Flow, Heat, and Nutrient Outflow at the Tagoro Submarine Volcano (Canary Islands, Spain)." *Science of the Total Environment* 918: 170565. https://doi.org/10.1016/j.scitotenv.2024.170565.

Maugeri, T. L., G. Bianconi, F. Canganella, et al. 2010. "Shallow Hydrothermal Vents in the Southern Tyrrhenian Sea." *Chemistry and Ecology* 26: 285–298.

McMurdie, P. J., and S. Holmes. 2013. "phyloseq: An R Package for Reproducible Interactive Analysis and Graphics of Microbiome Census Data." *PLoS One* 8: e61217.

Mériguet, Z., M. Vilain, A. Baudena, et al. 2023. "Plankton Community Structure in Response to Hydrothermal Iron Inputs Along the Tonga-Kermadec Arc." *Frontiers in Marine Science* 10: 1232923. https://doi.org/10.3389/fmars.2023.1232923.

Morel, F. M. M., and N. M. Price. 2003. "The Biogeochemical Cycles of Trace Metals in the Oceans." *Science* 300: 944–947.

Oksanen, J., F. G. Blanchet, M. Friendly, et al. 2019. "vegan: Community Ecology Package." v2.6.4.

Olins, H. C., D. R. Rogers, K. L. Frank, C. Vidoudez, and P. R. Girguis. 2013. "Assessing the Influence of Physical, Geochemical and Biological Factors on Anaerobic Microbial Primary Productivity Within Hydrothermal Vent Chimneys." *Geobiology* 11: 279–293.

Parada, A. E., D. M. Needham, and J. A. Fuhrman. 2016. "Every Base Matters: Assessing Small Subunit rRNA Primers for Marine Microbiomes With Mock Communities, Time Series and Global Field Samples." *Environmental Microbiology* 18: 1403–1414.

Park, M. G., W. Yih, and D. W. Coats. 2004. "Parasites and Phytoplankton, With Special Emphasis on Dinoflagellate Infections." *Journal of Eukaryotic Microbiology* 51: 145–155.

Price, R. E., and D. Giovannelli. 2017. "A Review of the Geochemistry and Microbiology of Marine Shallow-Water Hydrothermal Vents." In *Reference Module in Earth Systems and Environmental Sciences*. Elsevier.

Price, R. E., I. Savov, B. Planer-Friedrich, S. I. Bühring, J. Amend, and T. Pichler. 2013. "Processes Influencing Extreme as Enrichment in Shallow-Sea Hydrothermal Fluids of Milos Island, Greece." *Chemical Geology* 348: 15–26.

R Core Team. 2021. *R: A Language and Environment for Statistical Computing*. R Foundation for Statistical Computing.

Roda-Garcia, J. J., J. M. Haro-Moreno, L. A. Huschet, F. Rodriguez-Valera, and M. López-Pérez. 2021. "Phylogenomics of SAR116 Clade Reveals Two Subclades With Different Evolutionary Trajectories and an Important Role in the Ocean Sulfur Cycle." *mSystems* 6, no. 5: e0094421. https://doi.org/10.1128/msystems.00944-21.

Sambrook, J., and D. W. Russell. 2001. *Molecular Cloning: A Laboratory Manual*. 3rd ed. Cold Spring Harbor Laboratory Press.

Santana-Casiano, J. M., E. Fraile-Nuez, M. González-Dávila, E. T. Baker, J. A. Resing, and S. L. Walker. 2016. "Significant Discharge of CO_2 From Hydrothermalism Associated With the Submarine Volcano of El Hierro Island." *Scientific Reports* 6: 25686.

Santana-Casiano, J. M., M. González-Dávila, E. Fraile-Nuez, et al. 2013. "The Natural Ocean Acidification and Fertilization Event Caused by the Submarine Eruption of El Hierro." *Scientific Reports* 3: 1140.

Santana-Casiano, J. M., M. González-Dávila, and E. Fraile-Nuez. 2017. *The Emissions of the Tagoro Submarine Volcano (Canary Islands, Atlantic Ocean): Effects on the Physical and Chemical Properties of the Seawater*. IntechOpen.

Santana-González, C., J. M. Santana-Casiano, M. González-Dávila, and E. Fraile-Nuez. 2017. "Emissions of Fe(II) and Its Kinetic of Oxidation at Tagoro Submarine Volcano, El Hierro." *Marine Chemistry* 195: 129–137.

Schine, C. M. S., A.-C. Alderkamp, G. van Dijken, et al. 2021. "Massive Southern Ocean Phytoplankton Bloom Fed by Iron of Possible Hydrothermal Origin." *Nature Communications* 12: 1211.

Serôdio, J., and J. Lavaud. 2020. "Diatoms and Their Ecological Importance." In *Life Below Water. Encyclopedia of the UN Sustainable Development Goals*, edited by W. Leal Filho, A. M. Azul, L. Brandli, A. Lange Salvia, and T. Wall, 1–9. Springer International Publishing.

Skovgaard, A., S. Karpov, and L. Guillou. 2012. "The Parasitic Dinoflagellates *Blastodinium* spp. Inhabiting the Gut of Marine, Planktonic Copepods: Morphology, Ecology, and Unrecognized Species Diversity." *Frontiers in Microbiology* 3: 305.

Sotomayor-García, A., J. L. Rueda, O. Sánchez-Guillamón, et al. 2023. "Impact of Tagoro Volcano Formation on Benthic Habitats and Associated Biota: A Review." In *El Hierro Island*, edited by P. J. González, 217–239. Springer International Publishing.

Sotomayor-García, A., J. L. Rueda, O. Sánchez-Guillamón, et al. 2020. "Chapter 51 – Geomorphic Features, Main Habitats and Associated Biota on and Around the Newly Formed Tagoro Submarine Volcano, Canary Islands." In *Seafloor Geomorphology as Benthic Habitat*, edited by P. T. Harris and E. Baker, Second ed., 835–846. Elsevier.

Stoeck, T., D. Bass, M. Nebel, et al. 2010. "Multiple Marker Parallel Tag Environmental DNA Sequencing Reveals a Highly Complex Eukaryotic Community in Marine Anoxic Water." *Molecular Ecology* 19: 21–31.

Suzuki, R., Y. Terada, and H. Shimodaira. 2019. "pvclust: Hierarchical Clustering With P-Values via Multiscale Bootstrap Resampling." v.2.

Tarasov, V. G. 2006. "Effects of Shallow-Water Hydrothermal Venting on Biological Communities of Coastal Marine Ecosystems of the Western Pacific." *Advances in Marine Biology* 50: 267–421.

Tarasov, V. G., A. V. Gebruk, A. N. Mironov, and L. I. Moskalev. 2005. "Deep-Sea and Shallow-Water Hydrothermal Vent Communities: Two Different Phenomena?" *Chemical Geology* 224: 5–39.

Tilliette, C., F. Gazeau, G. Portlock, et al. 2023. "Influence of Shallow Hydrothermal Fluid Release on the Functioning of Phytoplankton Communities." *Frontiers in Marine Science* 10: 1082077. https://doi.org/10.3389/fmars.2023.1082077.

Vázquez, J.-T., O. Sánchez Guillamón, D. Palomino, et al. 2023. "Geomorphology of Tagoro Volcano Along Eruptive and Posteruptive Phases." In *El Hierro Island*, edited by P. J. González, 131–158. Springer International Publishing.

Wankel, S. D., L. N. Germanovich, M. D. Lilley, et al. 2011. "Influence of Subsurface Biosphere on Geochemical Fluxes From Diffuse Hydrothermal Fluids." *Nature Geoscience* 4: 461–468.

Weinstein, M. M., A. Prem, M. Jin, S. Tang, and J. M. Bhasin. 2019. "FIGARO: An Efficient and Objective Tool for Optimizing Microbiome rRNA Gene Trimming Parameters."

Wickham, H., M. Averick, J. Bryan, et al. 2019. "Welcome to the Tidyverse." *Journal of Open Source Software* 4: 1686.

Yu, G. 2020. "Using Ggtree to Visualize Data on Tree-Like Structures." *Current Protocols in Bioinformatics* 69: e96.

Yücel, M., S. M. Sievert, C. Vetriani, D. I. Foustoukos, D. Giovannelli, and N. Le Bris. 2013. "Eco-Geochemical Dynamics of a Shallow-Water Hydrothermal Vent System at Milos Island, Aegean Sea (Eastern Mediterranean)." *Chemical Geology* 356: 11–20.

Zhou, Z., P. Q. Tran, K. Kieft, and K. Anantharaman. 2020. "Genome Diversification in Globally Distributed Novel Marine Proteobacteria Is Linked to Environmental Adaptation." *ISME Journal* 14: 2060–2077.

Supporting Information

Additional supporting information can be found online in the Supporting Information section.